DEVELOPMENT OF A MATHEMATICAL MODEL FOR MIXING INDEX IN GAS – SOLID FLUIDIZED BED

A THESIS SUBMITTED IN PARTIAL FULFILLMENT
OF THE REQUIREMENTS FOR THE DEGREE OF

Master of Technology
in
Chemical Engineering

By

SUBAL CHANDRA RANA

Department of Chemical Engineering
National Institute of Technology
Rourkela
2007

DEVELOPMENT OF A MATHEMATICAL MODEL FOR MIXING INDEX IN GAS – SOLID FLUIDIZED BED

A THESIS SUBMITTED IN PARTIAL FULFILLMENT
OF THE REQUIREMENTS FOR THE DEGREE OF

Master of Technology
in
Chemical Engineering

By

SUBAL CHANDRA RANA

Under the Guidance of

Asst. Prof Dr (Mrs.) Abanti Sahoo

Department of Chemical Engineering
National Institute of Technology
Rourkela
2007

National Institute of Technology

Rourkela

CERTIFICATE

This is to certify that the thesis entitled, “Development of a Mathematical Model for Mixing Index in Gas-Solid Fluidized Bed” submitted by Sri Subal Chandra Rana in partial fulfillment of the requirements for the award of Master of Technology in Chemical Engineering with specialization in “Coal Chemical & Fertilizers” at the National Institute of Technology, Rourkela (Deemed University) is an authentic work carried out by him under my supervision and guidance.

To the best of my knowledge, the matter embodied in the thesis has not been submitted to any other University / Institute for the award of any Degree or Diploma.

Date

Asst. Prof Dr(Mrs.) Abanti Sahoo
Dept. of Chemical Engg.
National Institute of Technology
Rourkela – 760008

ACKNOWLEDGEMENT

I wish to express my sincere thanks to my guide, Dr (Mrs.) Abanti Sahoo for her able guidance and advices during my project work. Thank you for your patience and understanding. I must also acknowledge the HOD, Dr. P. Rath, faculty adviser Dr. K.C. Biswal and PG Coordinator, Dr. S.K. Agarwal for given this excellent opportunity to complete it successfully.

Subal Chandra Rana

CONTENTS

Abstract

Gas-solid fluidized beds have found wide industrial applications compared to fixed beds due to low pressure drop and good solid fluid mixing. Some of the important applications of gas–solid fluidized beds are in dairy, cement, food, and pharmaceutical industries for varied operations which include drying, cooling, coating and agglomeration. This permits a continuous automatically controlled operation with ease of handling and rapid mixing of solids leading to near isothermal conditions throughout the bed, thereby minimizing overheating in case of heat sensitive products. Mixing of solids is a common processing step widely used in industry. It is extensively employed in the manufacture of ceramics plastics, fertilizers, detergents, glass pharmaceuticals, processed food and cattle feed and in the powder metallurgy industry. Mixing index concept is a very much important factor in fluidization. Mixing index is the ratio of fraction of jetsam in the top portion of bed to the fraction in a well-mixed bed. Mixing index's value from 0 to 1 corresponds to complete segregation and complete mixing respectively.

A mathematical model of a real chemical process is a mathematical description which describes experimental facts and establishes relationship among the process variables. Mathematical modeling is an activity in which qualitative and quantitative representation or abstractions of the real process are carried out using mathematical symbols. In building a mathematical model, a real process is reduced to its bare essentials, and the resultant scheme is described by a mathematical formalism selected according to the complexity of the process. The resulting model could be either analytical or numerical in nature depending upon the method used for obtaining the solution. It is important that the model should also represent with sufficient accuracy qualitative and quantitative properties of the prototype process and should adequately fit the real process. For a check on this requirement, the observation made on the process should be compared with predictions derived from the model under identical

conditions. Thus, a mathematical model of a real process is a mathematical description combining experimental facts and establishing relationships between the process and variables.

Mixtures of solid particles of different sizes and/or densities tend to separate during fluidization. Particles that sink to the gas distributor are referred to as jetsam, while those that float on the fluidized bed surface are referred to as flotsam. Mixing and Segregation behavior of mixture particles is of practical importance because particle distributions in the fluidized bed influences the chemical reaction, bed expansion, and various mass and heat transfer properties in the fluidized beds.

Many studies have been made in the past in order to understand the underlying mechanisms and predict the behaviour of mixing and segregation, including the investigation of factors affecting the mixing/segregation, the development of predictive empirical and theoretical correlations, as well as mathematical and numerical models.

A theoretical model has been developed on the basis of " counter flow solid circulation model" .Considering both vertical and horizontal movement of the jetsam particles as some particles displace horizontally due to the bursting of bubbles , the dispersion model in the form of the differential equation is written and this is solved by finite difference method. For calculating concentration of jetsam particles and mixing index at any height of the bed ,a c-language program is written. The numerical results are in satisfactory agreement with experimental data. It is observed that both the concentration of the jetsam particles and mixing index decreases with the height of particles layers in the bed (measured from the distributor).It is also observed that the unpromoted bed gives better mixing index values than promoted bed due to its greater flow area. Optimum fraction of bed materials with respect to its distribution ion the upward and downward streams during the fluidization process can be taken up to 20%.When static bed height , operating fluidization velocity and jetsam particles composition values increases, for all the cases corresponding mixing index values decreases . It is seen that mixing index values of disc promoted bed and rod promoted fluidized bed are nearly same although flow area of rod promoted fluidized bed is greater than disc promoted fluidized bed.

LIST OF FIGURES

LIST OF TABLES

Chapter 1

INTRODUCTION

CHAPTER 1

INTRODUCTION

Gas-solid fluidized beds have found wide industrial applications compared to fixed beds due to low pressure drop and good solid fluid mixing. Some of the important applications of gas–solid fluidized beds are in dairy, cement, food, and pharmaceutical
industries for varied operations which include drying, cooling, coating and agglomeration. This permits a continuous automatically controlled operation with ease of handling and rapid mixing of solids leading to near isothermal conditions throughout the bed, thereby minimizing overheating in case of heat sensitive products.

Mixing of solids is a common processing step widely used in industry. It is extensively employed in the manufacture of ceramics plastics, fertilizers, detergents, glass pharmaceuticals, processed food and cattle feed and in the powder metallurgy industry. In fact, this operation is almost always practiced with processing of particulate matter. We resort to mixing of solids to obtain a product of an acceptable quality or to control the rates of heat and mass transfer and the rate of chemical reaction.

Considerable work has been done with respect to mixing and segregation in gas-solid homogeneous an heterogeneous fluidized bed, which encompasses the broad aspect of bed dynamics, viz. the mechanism, the quantification of mixing –the mixing index , the segregation distance and segregation intensity. In addition, limited work has been done in baffled beds and in beds with modified distributors.

Mixing index concept is a very much important factor in fluidization. A critical practical mixer exists when a particular fluid velocity, segregation of the two species occurs. Complete mixing of two particles types occurs only when both the components have the identical terminal velocities, that is perfect mixing(zero segregation)occurs around $U_J \div U_F = 1$ .The degree of mixing has been quantified by the term mixing index by several investigator . With binary mixtures of particles of different density investigators also have

developed the correlation for mixing index .Mixing index is the ratio of fraction of jetsam in the top portion of bed to the fraction in a well- mixed bed. Mixing index's value from 0 to 1 corresponds to complete segregation and complete mixing respectively.

A mathematical model of a real chemical process is a mathematical description which describes experimental facts and establishes relationship among the process variables. Mathematical modeling is an activity in which qualitative and quantitative representation or abstractions of the real process are carried out using mathematical symbols. In building a mathematical model, a real process is reduced to its bare essentials, and the resultant scheme is described by a mathematical formalism selected according to the complexity of the process. The resulting model could be either analytical or numerical in nature depending upon the method used for obtaining the solution. A good model should reflect the important factors affecting the process, but must not be crowded with minor, secondary factors that will complicate the mathematical analysis and might render the investigation. It is important that the model should also represent with sufficient accuracy qualitative and quantitative properties of the prototype process and should adequately fit the real process. For a check on this requirement, the observation made on the process should be compared with predictions derived from the model under identical conditions. Thus, a mathematical model of a real process is a mathematical description combining experimental facts and establishing relationships between the process and variables.

Solid mixing is a common mixing operation widely used in different industries. In fact, this operation is almost always practiced wherever particulate matter is processed. This is strongly influenced by different motilities of the mixed components, which depend on the particle properties. However, in industrial solids mixing, it is often required to mix Particles differing widely in physical properties viz. size, density and / or shape. The role of particle size and density and the air flow rate on the segregation or demixing behavior in a gas-solid fluidized bed has already been reported by some author. The degree of axial mixing of particles in fluidized beds is important for many continuous or batch processes, and control thereof is desirable. In fluidized beds consisting of particles with different size and/or density a concentration profile will develop over the height of the bed at moderate gas velocities. Most of the investigators who discuss the problem of solid mixing in a fluidized bed, have assumed that the solid mixing stems from the random movements of the particles and this assumption has rarely been questioned. If it is correct it follows that solid mixing will occur

by inter-particle diffusion or eddy diffusion as in true fluids and bubble rise. Because of the bubble rise, some solid are seen flowing up and others flowing down the bed.

Generally, the gas fluidized beds have excellent and rapid mixing characteristics for non-segregating particle systems. Much effort, both experimental and theoretical, has been spent in explaining this feature However, in industrial solids mixing, it is often required to mix particles differing widely in physical properties viz., size, density and/or shape. The role of particle size and density and the air flow rate on the segregation or demixing behavior in a gas–solid fluidized bed has already been reported. Some authors have concluded that a fairly wide particle size difference can be tolerated while a small density difference leads to ready settling of the denser particles. A qualitative model for particle mixing in a gas fluidized bed has been developed by some authors based on four physical mechanisms viz., overall particle circulation, interchange between the wake and the bulk phases, axial dispersion and segregation.

Mixtures of solid particles of different sizes and/or densities tend to separate during fluidization. Particles that sink to the gas distributor are referred to as jetsam, while those that float on the fluidized bed surface are referred to as flotsam. Mixing and Segregation behavior of mixture particles is of practical importance because particle distributions in the fluidized bed influence the chemical reaction, bed expansion, and various mass and heat transfer properties in the fluidized beds.

Many studies have been made in the past in order to understand the underlying mechanisms and predict the behavior of mixing and segregation, including the investigation of factors affecting the mixing/segregation, the development of predictive empirical and theoretical correlations, as well as mathematical and numerical models.

Chapter 2

REVIEW OF LITERATURE

CHAPTER 2

REVIEW OF LITERATURE

2.1 About Mathematical modeling

A mathematical model of a real chemical process is a mathematical description which describes experimental facts and establishes relationship among the process variables. Mathematical modeling is an activity in which qualitative and quantitative representation or abstractions of the real process are carried out using mathematical symbols. In building a mathematical model, a real process is reduced to its bare essentials, and the resultant scheme is described by a mathematical formalism selected according to the complexity of the process. The resulting model could be either analytical or numerical in nature depending upon the method used for obtaining the solution [01].

The objective of a mathematical model is to predict the behaviors of a process and to work out ways to control its course. Depending on the process under investigation, a mathematical model may be a system of algebraic or differential equations or a mixture of both.

Mathematical modeling involves three steps:

* Formalization-- the mathematical description of the process under investigation.
* Development of algorithm of the process.
* Testing the model and the solution derived from it.

is classified under three different bases:

1. Variation of various independent variables
2. State of process
3. Type of process

This classification of mathematical modeling is done based on whether the process variables vary with time as and independent variables or with both time and space coordinates as independent variables.

2.1.1 Types of Models

Distributed parameter models

If the basis process variables vary with both time and space, or if these changes occurs only with space of dimensions exceeding unity, such process are represented by distributed parameter model, which are formulated as partial differential equation.

Lumped parameter models

Processes in which the basic process variables vary only with time are represented by lumped parameter models, which are formulated as ordinary differential equation.

Classification based on the state of the process

The primary objective of the cybernetics is to control a given system or process .As a consequence, a compete mathematical model is expected to describe relationship between the basic process variables under steady state condition (a static model) and transit condition(a dynamic model) .

(A) Static Model

A static or steady model ignores the changes in process variables with time. The construction of a static model involves the following steps:

Step1. Analysis of the process to establish its physical and chemical nature , its pobjec5ive, the governing equations describing a given class of process and also its specific feature s as unit process.

Step2. Identification an ascertaining of the input and out put variables of the process

(B) Dynamic Model.

The construction of a dynamic or unsteady-state model reduces to obtaining the dynamic characteristics of the process, i.e., establishing relationships between its main variable as they change with time.

Dynamic characteristics can be obtained by theory, experiment, or both. In obtaining dynamic characteristics experimentally, disturbances are applies to the input of a system and the time response to the disturbance is noted.

The dynamic model of a process may take the form of any of the following:

1. A set of transfer function relating the selected dependent variables to one of several independent variables.
2. Ordinary or partial differential equations derived theoretically and containing the entire necessary dependent and in dependent variables.
3. Equations derived for the various elements of the unit process that may be analyzed independently of one another.

Depending upon whether a given process is deterministic or stochastic, it may be represented by any one of the following model

1. An analytical rigid model
2. A numerical rigid model
3. An analytical probabilistic model
4. A numerical probabilistic model.

(C) Rigid or deterministic models

These models usually describe deterministic process without the use of probability distributions. As mentioned above, the sub classification of rigid model is analytical rigid model and numerical rigid model, depending on whether the solution is obtained analytically or numerically.

(D) Stochastic or probabilistic models

These models usually represent stochastic (random) process. Here again the sub classification of probabilistic is analytical probabilistic (or stochastic) and numerical probabilistic (or stochastic model), depending on whether the solution is obtained analytically or numerically.

2.2 Previous Work

2.2.1 Mixing and segregation in fluidization

It is generally recognized that particle mixing well and rapidly when fluidized. A bed may be fluidized in the sense that all the particle are fully supported by the gas, but may still be segregated in the sense that the local bed composition does not correspond with the overall bed average[02]. Segregation is an in escapable by product of flow. It also negates the effect of mixing to the point that one may find cases of optimal mixing times. Segregation is likely to occur when there is substantial difference in the drag /unit weight between different particles. Particles having a higher drag/unit weight migrate to the distributor [03]. However if some particles are larger or denser than the others, they may settle to the bottom or at least be reluctant to mix. Paradoxically this excellent mixing system can bring absolutely excellent segregation. Therefore when particles with different density and size are fluidized, generally the particles tend to segregate. This phenomenon has been observed in both liquid and gas fluidized beds.

The combination of particles sizes, density and Shapes, has may be found in such fluidized beds is more or less infinite, but great insight into their general behavior can be found in from studying the binary or higher order systems. Mixtures of solid particles can separate or segregate while they are being handled. Out of the various mechanism of segregation, shifting of fines through a matrix of coarse particles [04], is the most important and common one. Whenever the fluidized bed particles vary in size or density (i.e. either the homogeneous or heterogeneous mixtures) and the gas flow rate exceeds the critical velocity, they tend to segregate in a vertical direction by forming the altering vertical bands of coarse bands of fine particles [05]. Initial investigations into segregation concentrated on density difference where Nienow and Cheesman[06], and Nienow and Chiba[07], introduced the terms flotsam and jetsam to describe the solids which occupy respectively the top and bottom of the bed. In a combined density/size situation the denser component generally behaves as

jetsam [08]. The less dense and /or smaller particles tend to move upward (which is called flotsam) relative to those that are denser and /or larger particles (called jetsam) which tend to move downward. In binary systems of size/or density, mixing is achieved by the rising bubbles, whose associated wake and drift action provoke an upward motion of particles. Particles descend in the bubble free regions thus resulting in an overall solid circulation .The same bubbles now cause segregation when the denser or larger particles tend to fall preferentially through the distributed region behind each bubble . Even denser or larger particles carried up in the bubble wake from the bottom segregated layer will be shed from the wake and descend rapidly,[09] .According to Rowe et al[10], the main segregation mechanism on particle system of equal density is due to particles falling through the free space of the bubble. Fan and Chang,[11] studied the fluidization and solid mixing characteristics of very large particles where bubble or slug induced drift and gross solid circulation appeared to be predominant solid mixing mechanisms. In many industrial situations where particles of different size and /or density are moving relative to each other a dynamics, dynamics equilibrium, is set between the competitive mechanism of mixing and segregation. This leads to a variation in solid composition over the height of the bed with some component – the flotsam tending to rise and others- the jetsam tending to sink .When two powders differing in size or density are fluidized are by gas, they segregate in a characteristic way. The upper part of the bed attains a fairly uniform composition, while the component, which tends to sink (jetsam) forms a concentrated bottom layer. The concentration of jetsam in the upper constant composition region compared with its overall value is a good measure of the degree of mixing observed. Mixing Index varies from zero for complete horizontal segregation to one for complete mixing. A. C. Hoffman [12] have investigated the particle dynamics in fluidized beds and found that incorporating a series of sieves like baffles in the bed, the natural tendency for segregation is enhanced .The phenomenon of segregation is nonlinear in nature: once it is started, it will lead to a decrease in bubble activity in the bed, this will in turn further decrease the mixing .Use of baffles influences the axial mixing of particles in a fluidized bred. It is well known that the main mixing mechanism in bubbling fluidized beds is the upward transport of jetsam particles in the wake of the rising bubbles(also, particle drift due to the movement of fluidization bubbles causes mixing)[13]

2.2.2 Variables effecting mixing and segregation:

From a practical point of view, a gas fluidized bed is usually assumed to be well mixed. However, segregation may occur when the bed contains more than one type /size of material. In that case, segregation will take place due to the differences in particle properties, such as particles densities size and shape. In general, segregation is more influenced by density difference. One of the main cause of the segregation is force imbalances on particles during the periodic disturbances (due to the density differences) associated with passage of the bubbles [06]. Further more other parameters that determine the extent of particle segregation in a fluidized bed system is related to the amount of particles used [02] .The characteristic parameter in this case is as follows:

1. The bed aspect ratio (H/Dc) at minimum fluidization, which is related to the total amount bed material.
2. The weight ratio of the segregating components in the bed
3. The Critical bed diameter(At which value the segregation is nil)
4. The properties of the fluidized bed system which are independent of particle properties. These include

(a) Fluidized bed dimension, such as the bed diameter and the height.
(b) The bed operating conditions such as superficial gas velocities.
(c) Position baffled, distributor and hole diameter and pitch and opening ratio of holes on the baffles as well as distributors.

Almost all investigators who discuss the problem of solid mixing in a fluidized bed have assumed that the solid mixing stem from the random movements of the particles and this assumption has rarely been questioned. If it is correct, it follows that solid mixing will occur by inter –particle diffusion or eddy diffusion as in true fluids [14]. Segregation has been studied extensively in static fluid beds and evaluating the effects of bed materials and fluid bed geometry. Richardson and Zaki [15] have observed the tendency for different size glass spheres to segregate in liquid –solid fluidized bed. Rowe et al [10], characterized segregation of mixtures with particles of different solids density in gas –solid fluidized beds. They were the first to refer the material that settled to the bottom as jetsam and that which floated to the top as flotsam .F or mixtures of solids with equal size but different densities, the flotsam is made up of lighter material, while the jetsam is the heavier solids; Nienow and Cheesman,[06];Nienow and Chiba,[07]. For mixtures of solids with

equal density but having either a wide size distribution or several discretely different size particles, the flotsam consists of the smaller and the jetsam the larger particles (Peeler and Huang,[16]; Nienow et al,[17]; Formisani,[18]; Wu and Baeyens,[02]. Mixing indices are defined based on the extent of segregation of different particles along the length of the fluid bed. Wen and Yu, [19] have reported that for a binary mixture a ratio of the minimum fluidization velocities greater than two ($U_J / U_F > 2$) is necessary for segregation. Rowe et al,[10] have found that in shallow beds the relative segregation in such mixtures is proportional to the ratio of the particle densities raised to the power 2.5 and the ratio of particle diameter to the power of 0.2. They also observed that adding of small amount of fines the Umf of the coarse materials considerably while a lot of coarse when added to fine alters the same with little effect. The previous investigations relating to the dynamics of mixed/segregated gas fluidized beds can be categorized under the following sub –heads:

1. Mechanisms of mixing and segregation
2. Quantification of mixing –the mixing index concept.
3. Segregation intensity and segregation distance.
4. Other related findings with respect to bed dynamics.
5. Effect of baffles and distributors on mixing and segregation.

2.2.3 Mechanism of mixing and segregation

Mixing and segregation occur simultaneously to produce an equilibrium distribution, which is essentially uniform in a horizontal plane but generally varies with the bed height. Both the process is influenced solely and entirely by the bubbles. Wooland and Potter,[20] have developed a technique for studying the solids movement associated with the rose of single bubble in a fluidized bed .Rowe et al,[10] have observed three different mechanisms, by which the particles mix or segregate and all are associated with bubbles. They used two different kinds of near spherical particles, using the pairs that differed in size, density or in both in a two dimensional as well as a cylindrical bed. At the equilibrium, the composition of the bed as a function of height was measured and the following correlations were proposed:

When size is considered

$$x = f(U - U_F) \times (d_j / d_f)^{-1/5} \quad \ldots\ldots\ldots\ldots\ldots\ldots (1)$$

When the density difference is considered

$$x = k(U - U_F) \times (\rho_j / \rho_f)^{-2.5}_{F} \qquad \text{..... (2)}$$

When k is proportionality constant.

The degree of mixing or segregation depends very much on the velocity. Even strongly segregating system can either be separated or well mixed by controlling this. Segregation varies as $(\rho_j / \rho_f)^{-2.5}$ and decreases as $(d_j / d_f)^{1/5}$. When there is an appreciable excess of jetsam the composition of the upper region is given by

$$x = f'(U - U_F) \times (d_j / d_f)^{-1/5} \times (\rho_j / \rho_f)^{-2.5} \qquad \text{..... (3)}$$

Where f' indicates the function of velocity. Above equation indicates that the effect of density ratio is considerable as compared to the size ratio .The main effect of size is to alter the U_{mf} of the mixture. Size difference alone leads to very little segregation in a fluidized bed.

Mixing of solids within a fluidized bed is caused mainly by the movement of bubbles. A bubble rises, solids close enough to the bubble enter into its cloud and are eventually drawn into its wake and complete mixing of solids occurs in the wake where movement is generated. This contributes partially to the lateral mixing of solids. In addition, a bubble causes a drift of particles to be drawn up as a spout below it. In a freely bubbling fluidized bed, wake fragments are periodically shed and replenished as the bubbles rise through the bed and there is a vertical displacement of the particles exclusive of the wake. At the bed surface, the bubble eruption induces lateral dispersion of part of the wake's particles over a large area, and the remainder of these particles is ejected into the freeboard. Solids mixing in a freely bubbling fluidized bed is caused not only by the vertical movement of bubbles and bursting of bubbles at the bed surface, but also by the lateral motion of bubbles as a result of the interaction and coalescence of neighboring bubbles. The lateral mixing of solids is augmented by the lateral motion of bubbles. In addition, the gross particles circulation or so-called 'Gulf Stream' is attributed to both vertical and lateral movement of bubbles, and is controlled by the distribution of bubbles.

Bubbling fluidized beds undergo extensive particle mixing, due to the motion of the bubbles themselves. However, under certain cooperating conditions,

segregation may take place. Either mixing or segregation may be desirable, depending upon the operation of the bed. Mixing, for instance, is more important in a gas–solids contact reactor such as those used in the chlorination of titanium bearing ores. For the reaction to proceed, the ore, coke, and gas must be sufficiently mixed so as to maximize product yields and minimize process times. Conversely, segregation is more important in classifiers where solids are to be separated based on size or density. The upward motion of bubbles through the bed of solids determines both the mixing and the segregation of particles, and is in accord with the two-phase theory of fluidization. As the bubble travels up through the bed, particles are drawn into a stagnant zone trailing the bubble called the wake. Axial mixing occurs as particles slough off the wake and new particles enter from the dense surrounding region. When the bubble reaches the top of the bed, the particles from the wake are deposited at the surface. By this mechanism, particles from the bottom of the bed may be mixed with those at the top. Meanwhile, the rising bubble leaves a void as it moves. This void is filled by particles falling down around the bubble. Those particles that tend to segregate to the bottom tend to fall just a little further and are referred to as jetsam. Particles that tend to accumulate at the top of the bed are called flotsam and fall less quickly. Mixing and segregation occur simultaneously, and at equilibrium the result of these processes is a concentration gradient in the axial direction while maintaining a fairly uniform distribution of particles radially .Solids that have a wide particle-size distribution have been shown to exhibit segregation due to differences in drag per unit weight . Particles of equal density exhibiting a higher drag per unit weight tend to behave as flotsam, while those with lower drag are jetsam. Generally, this results in larger particles accumulating at the bottom of the bed. However, particles of different densities are more likely to segregate than in systems with a wide size distribution. A number of mechanistic models have been proposed to describe the particle mixing and segregation phenomena. From these, several models have been developed to describe flotsam and jetsam concentrations at a steady-state condition. The model proposed by Gibilaro and Rowe [21] has been a popular starting point in estimating concentration profiles within a bubbling fluidized bed. In this model, solids in the bed are said to be distributed between two phases: the bulk phase, consisting of most of the solids, and the wake phase, containing the solids trailing the gas bubbles rising through the bed. Also, in this model, particles are said to consist of only two species: flotsam and jetsam. The model is developed by performing a mass balance on the flotsam in both phases (wake and bulk). The mass balance accounts for four mechanisms of particle transport: circulation, exchange, axial mixing, and segregation. Here, circulation is the movement of solids from the bottom of the bed to the surface via the

wake phase. The exchange mechanism is the movement of solids between the bulk phase and the wake phase as the bubbles rise in proportion to the concentration difference between the two phases. Axial mixing is defined as a pseudo-diffusion mechanism, a catch-all term to describe rising jetsam. However, Naimer et al. [17] concluded that this term could safely be dropped from the mass balance, since it does not account for any physically realistic mechanism in a fluidized bed. Finally, the segregation term is used to define the downward flow of jetsam. The rates of the remaining three mechanisms are related to bubbling through well-established hydrodynamic relationships rooted in the two-phase theory of fluidization.

2.2.4 Solids flow pattern and mixing kinetics

The solid flow patterns are examined first to generate some visual understanding of the segregation/mixing process. Spherical particles with different sizes can be represented with different radius circles. For a gas-fluidized system, the driving force for solid flow is the fluid drag force Therefore; the fluid drag forces acting on individual particles are calculated. To assist discussion, the fluid drag force is expressed as a dimensionless variable (the actual fluid drag force on a particle is divided by its gravity force). Starting from well-mixed packing, bed expansion is observed as soon as gas is injected. Segregation appears gradually. More and more flotsam particles move up to the top part of the bed. On the other hand, the jetsam particles move in the opposite direction. After a period of rearrangement of particles, a macroscopically stable or dynamical equilibrium state is reached. At this state, a nearly pure layer flotsam particle is seen in the top layer and keeps in fluidized state; while a de-fluidized layer in the bottom part is seen, which is rich in jetsam. Still, many flotsam particles are founding the bottom de-fluidized layer. At this given velocity, the fluidization of the top layer is not strong. The particles in the bed move more like those under gentle mechanical vibration with no significant bubbles or slugs. The cause of such a flow pattern can be better explained from the fluid drag forces on the particles in the bed. When gas injection starts, the fluid drag force is larger than the gravity force of flotsam and less than that of jetsam. Non-uniformity of the bed structure leads to two types of particle motion. First, the fluid drag force in some regions is large enough to lift not only the flotsam particles but also the jetsam particles above them, thus, all the particles can move up. Secondly, the flotsam particles in some regions are simply suppressed by their surrounding particles and stay at de-fluidized state. Both types of motion can be seen at velocity 0.7ms-1. The instant gas injection causes a bed expansion because it meets the minimum requirement

for fluidization. This leads to the upward motion of flotsam particles whose drag force is larger than their gravity force. With the arrangement of particles, the concentration of flotsam particles in the bottom part decreases, resulting in an increase of the minimum fluidization velocity and finally the formation of the de-fluidized layer. In the de-fluidized layer, the jetsam particles still receive a fluid drag force larger than their gravity, which are however not strong enough to breakthrough the suppression of jetsam particles. The flotsam particles are not uniformly distributed in the bottom layer. Some of them aggregate together by local fluidization or rearrangement. After a period of crunching with the top jetsam particles, a local fluidized region may increase and make the top jetsam particles unstable and eventually a path opened for the escape of the flotsam particles. This can be seen at 28.3 and 36.1s.When gas velocity is 0.8ms-1 , the motion of particles becomes a bit more vigorous, and segregation takes place quicker. After a period of evolution, a macroscopically stable state is reached. Similar to the case at gas velocity 0.7ms-1, fluidized and de-fluidized layers can be clearly observed. However, some difference exists. For example, the top-fluidized layer becomes more active and the concentration of flotsam particles in the de-fluidized layer decreases. The increased gas velocity will cause a larger fluid drag force for both flotsam and jetsam particles, hence a strong driving force for the upward motion of flotsam particles and a reduced suppression from the surrounding jetsam particles. Finally, a more significant segregation happens when the gas injection velocity is further increased to 0.9 and 1.0ms-1.

The upward motion of flotsam particles receives less suppression from the surrounding jetsam particles. A macroscopically stable state is reached even quicker. Two layers can be identified more distinctly. However, the concentration of flotsam in the bottom layer becomes smaller, and the top layer is in a stronger fluidized state where bubbles or slugs can be observed. In the bottom de-fluidized layer, the drag force acting on jetsam particles is very close to its gravity force. This makes the upward motion of flotsam particles easier and only a few flotsam particles are entrapped in the bottom layer. When the gas injection velocity is 1.2ms-1 the strong fluidization decreases the de-fluidized layer and more jetsam particles are involved in the top fluidized layer. This trend becomes particularly significant when gas velocity is 1.4ms-1, where the strong particle flow produces a better mixing state and only a very thin layer of jetsam particles are seen at the bottom the particle distribution is quite non-uniform. In a dense packing area, a strong drag force can often lead to the upward motion of particles. Following the bed expansion, the packing formed becomes loose and consequently, the drag force is decreased, which eventually causes the downward

motion of the particles under gravity. This cycle repeats to maintain a dynamically stable state. The final state of mixing/segregation is often expressed in terms of the relationship between composition and height, usually obtained by “bed-frozen” method. By taking into account the effects of front and rear walls, we have used this bed frozen technique to validate simulation method (Feng and Yu, 2004) [22]. This method is adopted here for quantitative analysis. The procedure is that gas supply is abruptly shut off to transform a bed from fluidized to fixed bed state, and the solid concentration in the fixed bed is then measured layer by layer. The concentration of jetsam decreases along the bed height from the bottom with the increase of gas velocity. When gas velocity is 1.0ms-1, the concentration of particles at this layer is almost constant, almost equal to 1.0ms-1.

The so-called modified Lacey mixing index is used for quantifying the mixing kinetics and the final degree of mixing. **Fig. 2** shows the variation of the mixing index with time at four gas velocities. Starting at the well-mixed packing state, the mixing index decreases as size segregation develops. At low velocities (e.g. 0.8ms-1), the rate of decrease is low. It takes about 50 s to reach a macroscopically stable state. With the increase of gas velocity (to, e.g. 1.0ms-1), the index decreases more rapidly and the final mixing index also decreases. A macroscopically stable state is reached in about 20 s. When gas velocity is further increased to 1.2ms-1, the mixing index increases corresponding to better mixing due to the stronger fluidization. At gas velocity 1.4ms-1, a stable state is reached rapidly and the mixing index just fluctuates at a high value representing even better mixing. Feng et al. (2004) [22] have showed that the initial arrangement of particles affects the segregation/mixing kinetics but not with the experimental results (Nienow and Chiba, 1981) [23]. But direct comparison is not appropriate because different conditions were used in their experimental and the present numerical studies.

Fig. 3 shows the variation of the mixing index with time at four gas velocities. Starting at the well-mixed packing state, the mixing index decreases as size segregation develops. At low velocities (e.g. 0.8ms-1), the rate of decrease is low. It takes about 50 s to reach a macroscopically stable state. With the increase of gas velocity (to, e.g. 1.0ms-1), the index decreases more rapidly and the final mixing index also decreases. A macroscopically stable state is reached in about 20 s. When gas velocity is further increased to 1.2ms-1, the mixing index increases corresponding to better mixing due to the stronger fluidization. At gas velocity 1.4ms-1, a stable state is reached rapidly and the mixing index

just fluctuates at a high value representing even better mixing. Feng et al. (2004) [22] showed that the initial arrangement of particles affects the segregation/mixing kinetics but not the final equilibrium state. Different gas velocities produce different degrees of mixing/segregation at such stable states. The time-averaged mixing index at each stable state for a given gas velocity can be determined. The results are shown in Fig.3. It is clear that the mixing index first decreases with the increase of gas velocity as a result of increased segregation. Then, with the further increase of gas velocity, it increases as a result of strong fluidization. A clear V shape curve can be seen. This curve depends on the size distribution of particles. This has been confirmed in our simulation using different volume fractions of jetsam, as shown in Fig. 3. This kind of V curve qualitatively agrees with the experimental work of Marzocchella et al. (2000) [24]

2.2.5 Quantification of mixing-The mixing index concept

Using particle mixture of difference size, shape and density, Wakeman and Stopp [25] identified the region of operation which gives rise to mixing of particles. Their observation is:

A critical particle mixture exists when, a particular fluid velocity, segregation of the two species occurs. Complete mixing of two particle types occurs only when both the components have the identical terminal velocities, i.e. perfect mixing (zero segregation) occur around $U_J / U_F = 1.0$. Above and below the line of perfect mixing the degree of mixedness of two species varies from 100% to nearly 0% in the upper region of the bed .According to them the segregation occurs at lower porosities of the bed.

Nienow et. al.[26] have proposed the correlations for the mixing index for an equal –size, density-variant binary mixture in three dimensional fluidized bed .For as size variant, equal density system of particles, mixing index proposed by Fan et.al.[27].The degree of mixing has been quantified by the term the mixing index by several investigators. With binary mixtures of particles of different density (i.e., heterogeneous materials) Nienow et.al. [06] have developed the correlation for the mixing index. For homogeneous binary mixtures Nienow et.al.have developed the correlation for an index of uniform mixing in terms of depth of penetration of large flotsam particles circulating in the bed as mentioned by the following correlation,

$$X/H = 0.12 (U - U_{mf})^{1/2} \quad \ldots\ldots\ldots\ldots\ldots\ldots (4)$$

It was also found by them that the ratio of actual circulation time to total journey time of large flotsam particle is an approximate measure of the averages depth of penetrations mentioned as under,

$$T_C / T = f(x/H) \quad \ldots\ldots\ldots\ldots\ldots\ldots\ldots (5)$$

Using solid mixtures (coal char, ash and silica sand) in a fluidized bed gasifier, Kawabata et.al. [28] have calculated the mixing index .For binary homogeneous and heterogeneous materials, Naimer et.al. [09] have estimated the parameters G and R model (expanded by Carson and Royal, [04] and linked the parameter to the physics of bubbling bed and to the particle properties with some modification for the mixing index .Wu and Baeyens [03] related the mixing and segregation properties of the homogeneous binary mixture system to the visible bubble flow rate and the particle size ratio. They have also developed an equation for the mixing index.

The mixing/segregation behavior of bi-sized particles in gas fluidization has been studied as a function of gas injection velocity by means of the discrete particle simulation. As an extension of the previous work (Feng et al., 2004) [22], this study uses gas velocity in a wide range to cover fixed, partially and fully fluidized bed conditions. Segregation/mixing behavior is analyzed in terms of flow patterns, solid concentration profile and mixing kinetics. The underlying mechanisms are elucidated in terms of the interaction forces between particles and between particles and fluid. In general, for a bed composed of bi-sized particles, there are three regimes corresponding to gas velocity. At low velocities, the bed stays as a fixed bed. At high velocities, it is fully fluidized producing good mixing of particles. Size segregation takes place in-between the two extremes, transforming an initially uniform bed into two layers: bottom de-fluidized layer rich in jetsam particles and a top fluidized layer rich in flotsam. As a transient process, segregation is strongly affected by gas velocity. There is a gas velocity producing the maximum segregation for a given mixture. Below this velocity, segregation increases and above this velocity, segregation decreases with the increase of gas velocity. The time to reach a macroscopically stable state can be up to tens of seconds, decreasing with the increase of gas velocity. The mechanisms governing the segregation can be explained in terms of interaction forces between particles and between particles and fluid. Segregation in the vertical direction takes place when the fluid drag force acting on flotsam is large enough to not only balance its gravity force but also break through

the suppression of the surrounding jetsam. It also changes the distribution of fluid drag forces and leads to the formation of a de-fluidized layer mainly composed of jetsam particles which may entrap some flotsam particles, and eventually the establishment of a macroscopically stable state. To reduce the degree of segregation, the interaction force between jetsam and flotsam must be high, to suppress the possible upward motion of flotsam particles at low gas velocities or help fluidize jetsam particles at high gas velocities. Both particle–fluid and particle–particle interactions vary spatially and temporally, giving very complicated behavior .Mixing and segregation, and fluidization and defluidization largely represent the complex dynamic balance of these forces either locally or globally. Future work is necessary to establish comprehensive understanding of the segregation/mixing process in relation to these forces under different flow conditions.

2.2.6 Mixing characteristics of Binary mixture

Generally, the gas fluidized beds have excellent and rapid mixing characteristics for non- segregating particle systems. Much effort, both experimental and theoretical, have been made in explaining this feature. However, in industrial solids mixing, it is often required to mix particles differing widely in physical properties viz, size, density and /or shape. This role of particle size and density and the air flow rate on the segregation or demixing behavior in a gas fluidized bed has already been reported .The previous author have concluded that a fairly wide particle size difference can be tolerated while a small density difference leads to ready settling of the dense particles. A qualitative model for particle mixing in a gas fluidized bed has been developed by Gibilaro and Rowe[28] based on four physical mechanism viz, overall particle circulation, interchange between the wake and the bulk phases, axial dispersion and segregation .the degree of axial mixing of particles in fluidized bed s is important for many continuous or batch process ,a control theory is desirable .In fluidized beds consisting of particles with different size and /or density , a concentration profile will develop over the height of the bed at moderate gas velocity. Most investigators, who discus the problem of solid mixing in a fluidize bed have assumed that the solid mixing stems from random movements of the particles and this assumption has been rarely questioned. If it is correct it follows that solid mixing will occur by inter – particle diffusion or eddy diffusion as in true fluids a bubble rise. Because of the bubble rise, some solids are seen flowing down the bed. This up flow and down flow of solids with an interchange between streams is basis for various counter –flow models. Solid exchange between a bubble wake and the emulsion

phase is one of the fundamental rate process that largely affect the direct mixing in fluidized beds. Work relating to the mixing of segregation particles in fluidize bed is scanty. Nicholson and Smith [29] have studied the axial mixing of particles differing in density in a fluidized bed proposed a first order rate equation to describe the progress of mixing in the short mixing time. Fan and Chang [11] have studied the fluidization and solid mixing characteristics of very large particles where bubble or slug induced drift and gross solid Circulation appeared to be the predominant solid mixing mechanism. By considering both horizontal and vertical dispersion of the particles along with the counter flow of solids and their circulation, a theoretical model has been proposed.

Based on developed model, concentration distribution of particles axially at different positions in the bed has been calculated. Also a different has been made for correlating the mixing index obtained experimentally with the various system parameters by means of dimensional analysis.

2.2.7 Models developed previously for axial solids mixing

A phenomenological model of axial solids mixing in a circulating fluidized bed is formulated. The model allows for main specific features of the process: ascending motion of particles in the core zone and their descending motion in the annular zone (inner circulation of solids); substantial changes of particle concentration, sizes of core and annular zones over the bed height; net circulation of solids and the effect of the bottom bed on the process. The validity of initial postulates is confirmed by comparison of calculated and experimental curves of mixing.

At present the technology of a circulating fluidized bed (CFB) is widely used in industry and power engineering [30, 31]. Due to comparatively small time of research, main regularities of heat and mass transfer in CFB have not been studied adequately which makes development and designing of new large-scale apparatuses with CFB difficult. This refers, to a full extent, to solids mixing the studies of which are of practical importance for processes where continuous treatment of particles (drying, .ring, combustion, etc.) is implemented or these particles gradually change their characteristics and require replacement (catalyst poisoning). Moreover, the character of solids mixing due to their 1000-fold higher bulk heat capacity, as compared with gas, determines the mechanism of heat transfer and leveling of temperatures in the apparatus. By virtue of known [30] special features of CFB

and its inner hydrodynamics (substantial non uniformity of particle concentration both over the riser height and in their horizontal cross-section, intense inner circulation of solids, etc.), the process of solids mixing in this system is rather complex for both experimental study and its mathematical modeling. Now, the literature contains only fragmentary data on the laws governing the process which is insufficient for quantitatively, and often qualitative, evaluation of the effect of different factors on the intensity of solids mixing. The main difficulty of investigations is in correct interpretation of the obtained experimental data which is directly connected with a rational choice of the physical model of the process. The simplest one-zone model with the only parameter —axial solids dispersion coefficient—was used in [32] for analysis of experimental solids residence time distributions in CFB with a diameter 0.152 and 0.305 m. A two-parameter model, which involves the particle velocity and axial solids dispersion coefficient, was used in [33] for analysis of the experiments on mixing of particles in CFB with a diameter 0.14 m. The authors do not give recommendations for determination of particle velocity. In [34], a more complex two-parameter two-dimensional (along the coordinates r and x) model which allows for a real structure of particle flows in CFB (ascending motion in the core zone and descending motion near the riser walls) and radial solids dispersion. The model considered a partial case of constant concentration of particles over the riser height, which considerable limited the range of its use. In [35], a rather complex multi parameter circulation model of solids mixing is suggested; the model directly allows for the two-zone structure of CFB. A considerable drawback of the model is in incorrect writing of diffusion and exchange terms which do not disappear at large times when the process of mixing ends and c1 ¼ c2 ¼ c1. It should be noted that this refers, to the same measure, to the above mentioned models where the form of presentation of diffusion terms follows from the Fick's law for systems with constant density. Since, as is known, CFB is a system where density changes substantially in both horizontal and vertical directions, the fact mentioned greatly restricts the applicability range of these models.

The main assumptions which form the basis of the model are the following:

1. Ascending particle motion with velocity u1 in the central part of the bed (core zone) and descending motion with velocity u2 in the annular zone form inner circulation of the solid phase. The following formulas are used for calculation of these velocities
[36, 37]

$$u_1 = u - u_t \quad \text{- - - - - - - - - - - - - - - - (6)}$$

$$u_2 = 0.1(u - u_t)Fr_t^{-0.7} \quad \text{- - - - - - - - - - - - (7)}$$

As is seen, velocities u1 and u2 are constant over the bed height.

2. The existence of outer (net) circulation of solids, which is produced by solids flow Js escaping from the upper part of the riser and then coming back to the bed base, is taken into account

3. In each horizontal cross-section of the riser there holds the equality

$$J_s = A\rho_1 u_1 - B\rho_2 u_2, \quad \text{……..… (8)}$$

which determines a value of the specific circulating particle flow Js (constant over the bed height and determining the intensity of net circulation of solids).

5. Local concentrations of particles in core zone (q1) and annular zone (q2) are linked by the correlation

$$\rho_2 = n\rho_1,$$

where n is the constant coefficient. By the data of [38],

$n \simeq 2\text{–}3.$

5. A mean (over the horizontal cross-section of the riser) density of the bed $\rho = A\rho_1 + B\rho_2$ is variable over the height and is described by an empirical formula

$$\frac{\rho'}{\rho_s} = \overline{J}_s(x')^{-0.82}, \quad H_0' \leqslant x' \leqslant 1. \quad \text{……..……..…..(9)}$$

6. Relative parts of the core zone (A) and the annular zone (B) change with the height, here in any horizontal cross-section of the bed

$$A + B = 1 \quad \text{…… (10)}$$

$$A = n\frac{u_2' + (x')^{0.82}}{u_1' + nu_2' - (x')^{0.82}(1-n)},$$

$$B = \frac{u_1' - (x')^{0.82}}{u_1' + nu_2' - (x')^{0.82}(1-n)},$$

for $H' \leqslant x' \leqslant 1$.

7. In the lower part of the bed there exists a zone with constant density and ideal mixing of particles—bottom bed. Its height is calculated by

$$H_0' = 1.25\,Fr_t^{-0.8}\bar{J}_s^{1.1}. \quad \ldots\ldots\ldots\ldots\ldots\ldots\ldots\ldots\ldots\ldots\ldots\ldots\ldots\ldots\ldots\ldots(11)$$

By the data of, bottom bed porosity weakly depends on the velocity of gas and is a rather stable quantity.

It is suggested to determine it by the formula

$$\varepsilon_{fb} = 1 - 0.33\,Fr_t^{-0.045}, \quad \ldots\ldots\ldots\ldots\ldots\ldots\ldots\ldots\ldots\ldots\ldots\ldots\ldots\ldots\ldots\ldots (12).$$

Particle exchange occurs between the core and annular zones. The exchange coefficient β_* is taken to be independent of the vertical coordinate x.

9. Dispersion transfer of marked particles with the coefficients D1 and D2 takes place in the core and annular zones, respectively, in addition to convective transfer.

10. Changes of the characteristics of CFB in horizontal direction are neglected. We first write the continuity equations for solids in the core zone and annular zones

$$\frac{\partial A\rho_1}{\partial t} + u_1\frac{\partial A\rho_1}{\partial x} = -A\beta_1\rho_1, \quad \cdots\cdots\cdots\cdots\cdots\cdots\cdots\cdots\cdots\cdots\cdots\cdots\cdots\cdots\cdots\cdots(13)$$

$$\frac{\partial B\rho_2}{\partial t} - u_2\frac{\partial B\rho_2}{\partial x} = A\beta_1\rho_1. \quad \cdots\cdots\cdots\cdots\cdots\cdots\cdots\cdots\cdots\cdots\cdots\cdots\cdots\cdots\cdots\cdots(14)$$

The quantity $A\beta_1\rho_1$ [1] allows for (within the framework of the one-dimensional model) the existence of a radial particle flow Jr from the core zone to the annular zone , which provides the experimentally observed decrease of densities ρ_1 and ρ_2 with a height at practically constant velocities u1 and u2. Having summed the above equations, the continuity equation obtained for the flow of outer circulation of solids

$$\frac{\partial \rho}{\partial t} + \frac{\partial J_s}{\partial x} = 0, \quad \ldots\ldots\ldots\ldots\ldots\ldots\ldots\ldots\ldots\ldots\ldots\ldots\ldots..(15).$$

According to Y Q Feng and A B Yu [39], a study of the mixing and segregation of particle mixtures in a gas-fluidized bed by means of a discrete particle simulation. Particle mixtures are composed of spherical particles with diameter 2mm for jetsam and 1mm for flotsam. The particles are initially packed randomly in a rectangular bed and then fluidized by gas uniformly injected at the bottom of the bed. The gas injection velocity varies to cover fixed, partially and fully fluidized bed conditions, in order to establish a full picture about the effect of gas velocity. Segregation/mixing behavior is analyzed in terms of flow patterns, solid concentration profile and mixing kinetics. It is shown that segregation, as a transient process, is strongly affected by gas velocity. There is a gas velocity producing the maximum segregation for a given mixture. Below this velocity, segregation increases and above this velocity, segregation decreases with the increase of gas velocity. The time to reach a macroscopically stable state can be up to tens of seconds, decreasing with the increase of gas velocity. The mechanisms governing the segregation and mixing of particles are elucidated in terms of the interaction forces between particles and between particles and fluid. Particle–fluid interaction initiates fluidization and segregation. Particle–particle interaction, however, also plays an important role in governing the segregation of particles. The degree of segregation results from the complex dynamic balance of the two interactions either locally or globally.

In recent years, discrete particle simulation has been developed and used to study various gas–solid flow behavior in gas fluidization (for example, Tsuji et al[40]; Hoomans et al.[41], 1996; Xu andYu,[42]; Mikami et al.,[43]; Kawaguchi et al., [44]; Ouyang and Li, [45]; Rong et al., [46]; Xu et al.,[47];Yuu et al., [48]; Zhang et al[49]; Rhodes et al.,[50]; Wang and Rhodes, [51]; Feng et al., [21]). The usefulness of this method lies in its capability of not only reproducing the flow patterns comparable to physical experiments but also giving quantitative particle scale information, such as the transient flow structure and interaction forces between particles and between fluid and particles. These authors analyzed the mixing/segregation behavior of particle mixtures in terms of flow patterns and mixing kinetics. Their results showed that the initial packing state of particles affects the segregation/mixing kinetics but not the final equilibrium state at a given gas velocity, and the degree of mixing/ segregation is strongly affected by gas velocity.

Significant segregation occurs when the gas velocity can only fluidize flotsam but not jetsam, and reasonable mixing occurs when the gas injection velocity is strong enough to fluidize the whole bed. Therefore, it is important to better understand the effect of gas velocity and its related mechanisms in terms of particle–particle and particle–fluid interactions.

Discrete particle simulation has undergone a period of model development since the pioneer work of Tsuji et al. [40], as discussed by Yu and Xu [52]. The model development has been further examined in previous work [Feng and Yun 21], with reference to the effects of model formulation, coupling schemes between the gas and solid phases, and different correlations to calculate particle–fluid interaction force. The validity of the approach has been verified against measurements under comparable conditions. Thus, below it is described of the model used for brevity. The solid phase is treated as a discrete phase that is described by a conventional discrete element method (DEM) (Cundall and Strack, [53]). Newton's second law of motion determines the translational and rotational motions of a particle at any time, t . It can be written as:

for translational motion :

$$I_i \frac{\mathrm{d}\omega_i}{\mathrm{d}t} = \sum_{j=1}^{k_i} \mathbf{T}_{ij} \quad \ldots\ldots\ldots\ldots\ldots\ldots\ldots\ldots (16)$$

Here mi , Ii , ki , $\mathbf{v}i$ and $\mathrm{w}iz$ are, respectively, the mass, moment of inertia, number of contacting particles, translational and rotational velocities of particle i; $\mathbf{f}f,i$ and $\mathbf{f}g,I$ are fluid drag force and gravitational force, respectively. $\mathbf{f}c,ij$, $\mathbf{f}d,ij$ and $\mathbf{T}i,j$ are the contact force, viscous contact damping force and torque between particles i and j . These inter-particle forces and torques are summed over the ki particles in contact with particle i. The contact force between particles and between particle and wall is calculated based on the soft-particle method. The particle–fluid interaction force is calculated according to the correlations by Di Felice [54] as recommended by Xu and Yu [42]. The gas phase is treated as a continuous phase and modeled in a way very similar to the one widely used in the conventional two-fluid model Gidaspow [55]. Thus, the governing equations are the conservations of mass and momentum in terms of the local mean variables over a computational cell, given by

$$\frac{\partial \varepsilon}{\partial t} + \nabla \cdot (\varepsilon \mathbf{u}) = 0 \qquad \ldots\ldots\ldots\ldots\ldots\ldots\ldots\ldots\ldots\ldots\ldots\ldots\ldots\ldots\ldots\ldots (17)$$

and

$$\frac{\partial (\rho_f \varepsilon \mathbf{u})}{\partial t} + \nabla \cdot (\rho_f \varepsilon \mathbf{u}\mathbf{u}) = -\nabla P - \frac{\sum_{i=1}^{k_c} \mathbf{f}_{f,i}}{\Delta V} + \nabla(\varepsilon \boldsymbol{\tau}) + \rho_f \varepsilon \mathbf{g}, \ldots\ldots\ldots\ldots\ldots\ldots\ldots\ldots\ldots\ldots (18)$$

where **u**, P and ρ_f are, respectively, the fluid velocity, pressure and density; τ, ε and ΔV are the fluid viscous stress tensor, porosity and volume of a computational cell; *kc* is the number of particles in the cell; and **g** is the gravity acceleration.

According to S. Barghi [56], the effects of size, shape, and density of tracer particles on mixing and segregation in liquid–solid fluidized beds were studied. A collision technique was used to define a new mixing index. Collisions between tracer particles and probes were found at 16 locations inside the fluidized bed simultaneously. The collision frequency of particles on probes was considered to be proportional to their local concentration inside the fluidized bed. Glass beads (3 and 5 mm in diameter) were used to study the effect of size on mixing. Graphite beads and cylindrical aluminum beads were introduced into a bed of spherical glass beads to investigate the density and shape effects, respectively. Smaller bed heights enhanced the mixing of particles lighter than the bed particles. Particle density had a greater effect on segregation than size and shape.

Particles are rarely entirely uniform in their characteristics in fluidized beds. Even in a fluidized bed of relatively uniform particles, the density, size, and shape of the bed particles may change due to collisions, attrition, growth of microorganisms (e.g., bioreactors), and reactions. These effects, as well as particle agglomeration, may cause a partial or complete segregation of particles, which strongly affects the bed performance. In case of complete mixing, the bed is a unique, well-mixed phase while in the complete segregation state—distinct layers of each of the solid species can be observed; but more often, the system undergoes an intermediate state between these two limits. In fact, both limits provide specific advantages such as staged chemical or physical separation and discharge of solids separately [67], or high degree of agitation to achieve higher efficiencies in chemical reactions. Therefore, the prediction of the behavior of a mixture in a fluidized bed is important for industrial operations.

In spite of extensive work on the mixing and segregation of binary mixtures in fluidized beds, the mechanism of mixing/segregation is still somehow incomplete and the predictions are essentially based on empirical correlations. In liquid–solid fluidized beds, liquid motion and hydrodynamic instabilities are the important factors in the mixing and segregation of particles. In an early work, the effect of particle size and density on axial mixing in liquid–solid fluidized beds was systematically investigated. The bed expansion and the prediction of local voidage in a fluidized bed containing two different particles are commonly represented by a serial model or a bed-in-series model. The model has been reported to be useful in the prediction of bed expansion for a partially/totally segregated bed of particles differing both in density as well as size. The concentration profile in a binary system can be estimated from the unit cell model. The dispersion model [57-59] was applied to the prediction of axial distribution of particles in a fluidized bed of particles with different sizes. In a mathematical model based on mass balance [60], density gradient measurement was used to obtain the concentration profile throughout the bed. Measurements of porosity profile [57], slip velocity [59], and pressure gradient [58, 67] were some other approaches to predict the concentration profile in liquid–solid fluidized beds using a dispersion model. The measurement of particle dispersion coefficient [61–63] was another attempt to show the concentration profile in a fluidized bed of different particles. In a recent study [71], an electromagnetic method was applied to study particle mixing by monitoring tracer particle trajectory in a bubbling fluidized bed. The method utilizes the interaction between a magnetic field imposed on a fluidized bed (by metallic rings) and a single tracer particle covered by metal moving inside the bed. A radioactive particle tracing technique has been applied in fluidized beds for the study of tracer particle trajectory and concentration profiles [72]. Empirical correlations [64, 65] have been presented for the prediction of axial concentration profiles and radial liquid dispersion coefficients [70] in liquid–solid fluidized beds of binary systems. In a binary mixture of particles having the same density in a liquid–solid fluidized bed, segregation occurred when the size ratio was greater than 1.56 [66]. In previous studies, the application of tracer particles in the study of hydrodynamics and concentration profiles in fluidized beds was limited to one tracer particle due to the experimental restrictions. In this study, a new simple, robust, and inexpensive method was applied, which measured collisions between tracer particles and probes inside the fluidized bed. The collisions are directly related to particle motion. Thirty tracer particles were introduced into the bed to have a better view of the particle concentration profile. The mixing and the segregation of particles are

described by measuring collisions between tracer particles of a given size, shape, and density, and special probes, which are distributed throughout the bed. Higher local collision frequencies correspond to regions where the concentration of tracer particles is high. In a perfectly mixed bed, the collision frequency would be the same for all probes; while in a completely segregated bed, some electrodes would register no collisions. An uneven distribution of the collision frequency indicates partial segregation.

A phenomenological model of solids mixing in a circulating fluidized bed is formulated by Yu.S. Teplitskii [73]. The characteristic feature of this model is taking into account the convective flows of particles in the radial direction, which provide the observed in practice essential decrease of the concentration of particles over the riser height. It is established by comparison of calculated and experimental curves of mixing that the value of the coefficient of radial dispersion of particles lies within the range 0.0006–0.006 m2/s.

As is known, solids mixing in the circulating fluidized bed (CFB) is a multifactor process taking place against the background of complicated inner hydrodynamics [74]. For the simulation of the phenomenon various calculation schemes were invoked which reflected, to some extent, the mechanisms of the real process of solids mixing in the CFB apparatuses. The proposed models can be arbitrarily divided into two groups. The first one includes the models of axial (longitudinal) mixing in which the determining quantities and concentrations are considered as depending on just the longitudinal coordinate. In [75], the critical analysis of such models is carried out and on the basis of it a rather simple two-zone model of axial solids mixing is offered which includes the equations:
for the core zone

$$\frac{\partial A\rho_1\bar{c}_1}{\partial t} + u_1\frac{\partial A\rho_1\bar{c}_1}{\partial x} = \beta_*\rho(\bar{c}_2 - \bar{c}_1) - A\rho_1\beta_1\bar{c}_1; \quad \ldots\ldots\ldots\ldots\ldots\ldots\ldots\ldots\ldots\ldots\ldots\ldots(19)$$

for the annular zone

$$\frac{\partial B\rho_2\bar{c}_2}{\partial t} - u_2\frac{\partial B\rho_2\bar{c}_2}{\partial x} = \beta_*\rho(\bar{c}_1 - \bar{c}_2) + A\rho_1\beta_1\bar{c}_1. \quad \ldots\ldots\ldots\ldots\ldots\ldots\ldots\ldots\ldots\ldots\ldots\ldots(20)$$

As is shown in [74], this model is able to adequately describe the experimental curves of mixing obtained for both the core zone and the annular zone. The second group represents the models where the transfer of marked particles in both the axial and radial direction is considered. In [75], the experimental data were interpreted on the basis of the two-dimensional non stationary model

$$\frac{\partial c^*}{\partial t} = D_a \frac{\partial^2 c^*}{\partial x^2} + \frac{D_r}{r}\frac{\partial}{\partial r}\left(r\frac{\partial c^*}{\partial r}\right) - \frac{\partial (v_s c^*)}{\partial x}, \quad \ldots\ldots\ldots\ldots\ldots\ldots\ldots\ldots (21)$$

which does not account for the convective motion of particles from the core zone to the annular zone. Probably, that is why the model can be applied only in the upper part of the CFB where the mechanism mentioned above is slackened and the concentrations of particles in both zones are practically independent of the height. The variation of the density over the CFB height is also not accounted in the model [77]:

$$\frac{\partial(\rho(r)c)}{\partial t} + \frac{\partial(J_s(r)c)}{\partial x} = \frac{D_r}{r}\frac{\partial}{\partial r}\left(r\frac{\partial(\rho(r)c)}{\partial r}\right), \quad \ldots\ldots\ldots\ldots\ldots (22)$$

where Js(r) is the value of the local mass flux of particles (positive in the core zone and negative in the annular zone). Model [77] reflects the two-zone structure of CFB and, as well as [76], it can be justifiably used only in the upper part of the bed. Besides, because of the wrong notation of the dispersion term it gives a physically absurd expression

$$\frac{c_\infty D_r}{r}\frac{\partial}{\partial r}\left(r\frac{\partial \rho(r)}{\partial r}\right) \neq 0 \text{ for } t \to \infty, \text{ when } c \to c_\infty = \text{const.} \quad \ldots\ldots\ldots (23)$$

Nevertheless as the authors of [77] state, this model adequately described the experimental data in the upper part (x = 4 m) of the 5-m riser. As is seen, the field of application of models [76] and [77] is limited. They can be used only in the upper zone of CFB, where q = const. Besides, it is important to note that in the models mentioned above there is no evident form of accounting for the most important mechanism of mixing – radial convection of particles which provides the observed in practice essential decrease of q1 and q2 with the height at practically constant longitudinal velocities u1 and u2. In the present work, two problems were posed: to account for the indicated mechanism of mixing thus

increasing the level of theoretical analysis and to develop on this basis the generalized model of the process which describes solids mixing over the whole volume of the riser of CFB.

Laihong Shen, Mingyao Zhang, Yiqian Xu[78] suggests that according to Kunii and Levenspiel [79] assumed that a free gas-solids fluidized bed consists of a dilute (bubble) phase (B) containing no solids and of two dense phases containing all the solids. The distribution of bubbles entering the bed is controlled by the uniformity of gas distribution and the distribution of orifices in the grid, and significantly by the size and height of the bed. Coalescence causes the mean bubble size to increase up the bed and also affects local bubble motion. Solids are moved upward by the action of bubbles via two mechanisms, wake and drift. It is considered convenient to lump solids motion through wake transport as well as drift in the wake fraction (W). There is a primary down flow of solids in the bed; the descending stream corresponds to the surrounding regions of rising bubbles, so that overall convective circulation is set up.

The upward moving dense phase (W) is in contact with the downward moving dense phase (E). Solids can exchange between the E and W phases. In the E phase, solids mixing along the radial or lateral direction are composed of two components, the first is the diffusion component generated by the random movement of solids, and the second is the convective component imparted by the lateral motion of bubbles as a result of the interaction and coalescence of neighbouring bubbles. Fan et al. [18] took into account lateral solids mixing in a stochastic model, determining a total lateral mixing coefficient as a sum of diffusive and convective coefficients. Therefore, solids mixing of the E phase along the radial direction can be described by means of a diffusion model.

Other relevant assumptions are as follows:

(a) Plug flow for gas is assumed through a fluidized bed.

(b) No entrainment of solids from the bed takes place.
(c) Volumetric fraction of the bubbles remains constant.
(d) Porosities of the dense phases remain equal and constant.

Figure-4 shows the schematic mass balance of the tracers at the position (x, y) of the bed in E and W phases.

The dynamic balances of the tracers are given by the following equations:

$$\frac{\partial C_W}{\partial t} + \frac{\partial (U_W C_W)}{\partial y} = -K_W (C_W - C_E) + q_1 - q_2 C_W \quad \ldots\ldots\ldots\ldots\ldots\ldots (24)$$

$$\frac{\partial C_E}{\partial t} - \frac{\partial (U_E C_E)}{\partial y} = \frac{\partial}{\partial x}\left(D_{ar} \frac{\partial C_E}{\partial x}\right) + f_w K_W \delta_B (C_W - C_E)/f_E + q_1 - q_2 \cdot C_E \quad \ldots\ldots\ldots\ldots\ldots\ldots\ldots\ldots\ldots (25)$$

where the volumetric fraction of bubble wakes is:

$$f_E = 1 - \delta_B - \delta_B f_w$$

and

$$q_1 = \frac{Q_1}{A_{feed}(1 - \delta_B)}$$

$$q_2 = \frac{Q_2}{A_{feed}(1 - \delta_B)\rho_S(1 - \epsilon_{mf})}$$

Initial and boundary conditions are:

(i) Initial tracer concentrations in the E and W phases are given.

(ii) Solids in the W phase arrive at the top of the bed and re-enter the bed through the down flowing E phase.

(iii) At the distributor, the solids in the E phase reenter the bed through the W phase. It is assumed that point samples of solids taken from the bed are average static mixtures (subscript d) of the emulsion phase (E) and the wake one (W)

where the volumetric fraction of bubble wakes is:

$$f_E = 1 - \delta_B - \delta_B f_w \quad \ldots\ldots\ldots\ldots\ldots\ldots\ldots\ldots\ldots\ldots\ldots\ldots\ldots\ldots (26)$$

and

$$q_1 = \frac{Q_1}{A_{feed}(1-\delta_B)} \quad \ldots\ldots\ldots\ldots\ldots\ldots\ldots\ldots\ldots\ldots\ldots\ldots\ldots\ldots (27)$$

$$q_2 = \frac{Q_2}{A_{feed}(1-\delta_B)\rho_S(1-\epsilon_{mf})} \quad \ldots\ldots\ldots\ldots\ldots\ldots\ldots\ldots\ldots\ldots\ldots\ldots\ldots\ldots (28)$$

$$C_d = \frac{\delta_B f_W C_W + (1-\delta_B - f_W\delta_B)C_E}{(1-\delta_B)} \quad \ldots\ldots\ldots (29)$$

As the dense phase porosity is constant throughout the bed, the upward flow rate of solids should be equal to the downward flow rate, as given below

$$\delta_B f_W U_W = f_E U_E \quad \ldots\ldots\ldots\ldots\ldots\ldots\ldots\ldots\ldots\ldots\ldots\ldots\ldots\ldots\ldots\ldots\ldots\ldots (30)$$

Bing Du, Fei Wei [80] have experimented an impulse injection phosphor tracer technique is proposed to study the effect of particle properties, including particle size, particle density and particle sphericity, on the lateral mixing behavior in a riser with FCC particles as fluidized materials. The RTD curves of all kinds of particles have one peak, which can be described by a two-dimensional dispersion model. Between 15 and 80 _m, the lateral solids dispersion coefficient may have a maximum value, indicating that there exists a minimum particle size at which the particles do not aggregate intensively in the riser. The lateral solids dispersion coefficient decreases with increasing particle density and solids concentration, while increasing with increasing particle sphericity and superficial gas velocity. A correlation is developed to account for the influence of particle properties, operating conditions on the lateral dispersion coefficient, which fits the experimental data well.

G. Grasa, J. C. Abanades [81] have studied that two widely used models to describe axial solid mixing in fluidized beds (the dispersion model and the countercurrent back mixing (CCBM) model) are evaluated against identical sets of experimental data. Experimental work has been obtained at different conditions (gas velocity, particle properties and two column diameters) using an image analysis technique. Previously published data by

other authors are also compiled to enlarge the experimental database for model development and validation. It is shown that both models are capable to 5t the majority of experiments well, in agreement with a well-known relation between the models in some extreme conditions. This relation is further explored by incorporating independent measurements of the tracer rise velocities during the mixing experiments. It is concluded that, although a simple correlation for the solid dispersion coe8cients compiled in this work is useful, the CCBM model is a much more reliable idealisation in describing and scaling up axial solid mixing in fluidized beds.

I. Eames, M. A. Gilbertsonhad [82] have studied about one of the attractive features of bubbling gas-fluidized beds are that they mix particles well. Fluidized beds of fine particles allow high levels of heat and mass transfer between the particles and have uniform properties because of the good mixing driven by the voids, or bubbles, in them. Early gas-fluidization research was instrumental in developing the general concepts that can be used to obtain practical estimates of mixing and transport in a fluidized bed. Some of these concepts have been absorbed and taken forward by other areas of multiphase flows. It is therefore timely to review these approaches and describe their (re)application to gas-fluidized beds, in light of recent studies which relate drift and dispersion.

They showed that there are three dominant physical processes in the bulk of the bed that cause mixing: first, particles are transported up with the vortices (these are often referred to as traveling in the F wake_ of the bubble); secondly, the permanent displacement or drift of the particles outside the bubble; thirdly, there is the return flow of particles in the bed to compensate for those displaced upwards by the bubbles. These different mechanisms can be seen: the dark lobe-like trails are particles that have been entrained by the bubbles and transported upwards; the peak of dark particles is a result of drift, the distortion induced in the horizontal interface between differently coloured particles by the return flow is apparent. The experiments did not show any mixing in the bed that was not generated directly from the passage of a bubble [9].

A framework commonly used for describing mixing in fluidized beds was laid out by Kunii and Levenspiel [79]. A starting point is the specification of a diffusion equation describing the transport of passive material. To close these equations, diffusion and advection coefficients are specified, often by fitting experimental data however,

it is clear that much of the mixing in fluidized beds is driven by the currents generated by the bubble movement. To take this into account, the Counter-Current Back mixing Model (CCBM) was developed which divides the particles in the bed between the portion traveling upwards with the bubbles and the remainder transported downwards as a return flow, with an exchange between the two groups of particles. The exchange coefficients are also found from empirical fits. These approaches have been compared with each other [81], and also combined. A further development is the explicit modeling of the convection of the particles, and the connection of this with diffusion and exchange coefficients [83-85]. Different methods can be used e.g. [86], but the physical picture is the same. The results can be useful practically, but rely greatly on empiricism [81]. Experimental measurements show that in most of the bed, mixing is dominated by the vertical transport of particles which may be characterized by vertical particle dispersivity, D (p). While a number of attempts have been made to connect physically the vertical dispersivity with some aspect of the bubbles, this is often imprecise. Most attention has focused on the entrainment of particles by the bubble wakes – an area of agitated flow at the base of the voids – as suggested by Kunii and Levenspiel [79]. Rowe's experiments demonstrated that entrained material is redistributed throughout the void and gradually exchanged with the ambient material as the bubble rises. These accords with the model of Batchelor and Nitsche [87] where a vortex takes time to empty of particles. Furthermore, particles initially outside the vortex do not necessarily pass straight through it, but may circulate several times before leaving. During this time the particles will be transported by the bubble and so will undergo a significant vertical displacement. Rowe et al.'s experiments [9] suggest that this contribution to mixing is often not as significant as that induced by drift. In some cases, other processes, such as drift, are invoked but their treatment is the same as that for the wakes with the use of exchange coefficients. At present, the connection between the drift induced by an isolated bubble, addressed by Rowe et al. [9], and the mixing induced by collections of bubbles has not been made.

Bubbles also play important roles in mixing. According to Prof. G .K. Roy and A. Kumar [88], a turbulent promoter in gas-solid fluidized bed has been found to be effective in controlling the bubble behavior that is hindering the formation and growth of bubbles, and limiting their sizes and thereby delaying bubbling and slugging. The use of promoters would arrest bubble growth, re-distribute the gas and improve the homogeneity of the fluidized bed. In the present study, the effect of rod, disk and blade type of promoters on

bubble behaviour and slug formation in case of gas-solid fluidized beds have been examined and compared with the conventional un-promoted bed. Kono and Jinnai1[89] have reported that the bubble sizes can be kept significantly smaller than those in the conventional beds and maintained almost constant regardless of the bed height. Xiaogang and Heqing [90] have observed the effect of operating conditions on bubble behaviour in a fluidized bed with perforated promoters and resolved that for the same superficial gas velocity, bubble frequency and rise velocity are independent of aperture ratio, hole dia (baffle plate) and baffle plate distance. In gas-liquid or gas-liquid solid contacting devices, Tsuchiya and Fan [91] have explained that the bubble coalescence and breakup play a crucial role in determining the distribution of bubble size and rise velocity and gas-liquid interfacial area.

Geldart [4] have suggested a correlation for minimum bubble velocity as

$$U_{mb} = K_{mb}\,\bar{d}_s \qquad \ldots\ldots\ldots\ldots\ldots\ldots\ldots\ldots (31)$$

where

$$\bar{d}_s = 1/\sum_i \left(\frac{X_i}{d_{si}}\right)$$

and Kmb is the constant whose value is 100 (in CGS system). The large contrast in stability between gas and liquid fluidized beds is related to the presence of bubbles in most of the gas fluidized beds and their absence from most liquid-fluidized beds. Hence, the gas-fluidized bed is associated with the rapid growth of instability with bubble formation. Davidson and Harrison [5] have observed that the interval between minimum bubbling velocity and minimum fluidization velocity represents the stable uniform fluidization, which shrinks rapidly as the size of the particles increases. Rowe [6] proposed a correlation to predict bubble size in a gas solid fluidized bed (when size is not restricted by the column dimension) as

$$d_b = \frac{\left(U_f - U_{mf}\right)^{1/2}\left(h + h_o\right)^{3/4}}{g^{1/4}} \qquad \ldots\ldots\ldots\ldots\ldots (32)$$

where $\left(U_f - U_{mf}\right)$ is the excess gas velocity.

Darton, et.al. [7] have suggested another correlation for bubble size and the same is represented as

$$d_b = \frac{0.54\left(U_f - U_{mf}\right)^{0.4}\left(h + \sqrt{\frac{A_c}{n}}\right)^{0.8}}{g^{0.2}} \quad \ldots\ldots\ldots\ldots\ldots(33)$$

Bubbles formed at the distributor, coalesce in the normal way until they reach the size of a slug. Stewart and Davidson [8] have stated that at superficial gas velocity below the following bubble rise velocity, slugging should not take place

$$U_{ms} = U_{mf} + 0.07\sqrt{gD_c} \quad \ldots\ldots\ldots\ldots\ldots\ldots\ldots\ldots(34)$$

The bed must sufficiently be deep for coalescing bubbles to attain the size of a slug. Baeyens and Geldart [92] have felt that the above condition is applicable

Only if $h_{mf} > 1.3\,D_c^{0.175}$ in SI units, otherwise the minimum slugging condition is expressed as

$$U_{ms} = U_{mf} + 0.07\sqrt{gD_c} + 0.16\left(1.3\,D_c^{0.175} - h_{mf}\right)^2 \quad \ldots\ldots\ldots\ldots(35)$$

It has been found that the minimum bubbling velocity depends on particle dia and the bed properties. Further, it has been observed that for the same particle size, minimum bubbling velocity is minimum in case of un-promoted bed followed by beds with disk and rod promoters and the maximum in the case of bed promoted with blade type of promoter. This observation can be explained in terms of peripheral contact of the bed geometry with the fluid. In case of un-promoted bed, the periphery of column only is in contact with the fluid flow and give minimum peripheral contact resulting minimum bubbling velocity. In case of promoted beds, the surfaces of the promoter also contribute to periphery and hence more peripheral contact with the fluid flow. The maximum peripheral contact is in the case of bed with blade type of promoter followed by beds with rod and disk promoters. The maximum peripheral contact in the case of bed with blade type of promoter results in maximum bubbling velocity. In other words, bubble formation is delayed in the case of bed having more peripheral contact with the fluid flow.

Chapter 3

MODELING FOR MIXING

CHAPTER-3
MODELING OF MIXING INDEX

3.1 Modeling for mixing

Most of the engineering process that demand accurate product quality, and proceed at high rates, high temperature and high pressures, are distinct for their utmost complexity. A simple change in one of the variables may bring about complex and non-linear changes in other variables.

The external potential of information about any engineering process is extremely high. This complex situation can be handled diligently with very narrow channels of perceptions by gaining an insight into a particular process using models. A model is simplified representation of those aspects of an actual process that are being investigated. In a simplified form a model of the system can be defined as the mathematical representation of the physical and chemical phenomena taking place in it which is used to analyze the behavior of a chemical process.

The flow information is broken down into two stages. In the first stage, the model is compared with the real process and considered adequate if the discrepancy is negligible. This procedure is called modeling .Or in other words the activities leading to the development of the model is referred to as modeling. Modeling is subdivided into groups:

1. Physical modeling
2. Mathematical modeling

The specific application s of Mathematical modeling in chemical process are generally referred to as chemical system modeling.

3.2 Mathematical Modeling for Mixing Index

Mathematical modeling is very much an art. It takes experience, practice, and brain power to be a good mathematical modeler. Mathematical model of a real chemical

process is a mathematical description which combines experimental facts and establishes relationships among the process variables. Mathematical modeling is an activity in which qualitative and quantitative representations or abstractions of real process are carried out using mathematical symbols. In building a mathematical model, a real process is reduced to its bare essential and the resultants scheme is described by a mathematical formalism selected according to the complexity of the process. The resulting model could be either analytical or numerical in nature depending upon the method used for obtaining the solution [03]. The objective of a mathematical model is to predict the behaviors of a process and to work out ways to control its course. Depending on the process under investigation, a mathematical model may be a system of algebraic or differential equations or a mixture of both.

A good model should reflect the important factors affecting the process, but must not be crowded with minor, secondary factors that will complicate the mathematical analysis and might render the investigation. It is important that the model should also represent with sufficient accuracy qualitative and quantitative properties of the prototype process and should adequately fit the real process. For a check on this requirement, the observation made on the process should be compared with predictions derived from the model under identical conditions. Thus, a mathematical model of a real process is a mathematical description combining experimental facts and establishing relationships between the process and variables.

3.3 Use of mathematical model

Without doubt, the most important result of developing a mathematical model of a chemical engineering system is the understanding that is gained of what really makes the process “tick”. This insight enables one to strip away from the problem the many extraneous “confusion factor” and to get to the core of the system. One can see more clearly the cause-and-effect relationship between variables. Mathematical models can be useful in all phases of chemical engineering, from research and to plant operations, and evening business and economic study. Most of the investigators who discuss the problem of solid mixing in a fluidized bed, have assume that the solid mixing stems from the random movements of the particles and this assumption has rarely been questioned .If it is correct, it follows that solid mixing will occur by inter particle diffusion or eddy diffusion as in true fluids and bubble rise .Because of the bubble rise, some solid are seen flowing up and other

flowing down the bed. This up-flow and down-flow of solids with an interchange between streams is the basis for various counter flow models.

3.4 Development of mathematical model for mixing index

It is a well known fact that some solids flow up and others flow down during fluidization in a gas –solid fluidized bed .This up-flow and down –flow with an interchange between the streams is the basis for various counter flow models that have been proposed account for the vertical mixing of solids. Van Deemter[93] have divided the solids into two streams for a tall enough bed of solid particles and developed the following models.
For the up-flowing models:

$$f_u\left(\frac{\partial C_{su}}{\partial t}\right) + f_u u_{su}\frac{\partial C_{Su}}{\partial z} + K_S(C_{su} - C_{sd}) = 0 \ldots\ldots\ldots\ldots\ldots\ldots\ldots \text{(36)}$$

For down flowing streams:

$$f_d\left(\frac{\partial C_{sd}}{\partial t}\right) + f_d u_{sd}\frac{\partial C_{sd}}{\partial z} + K_S(C_{sd} - C_{su}) = 0 \ldots\ldots\ldots\ldots\ldots\ldots\ldots \text{(37)}$$

The author also showed that the changes in concentration of labeled solids could be represented by an effective dispersion coefficient given by

$$D_{Sv} \cong \frac{f_d^2 u_{sd}^2}{K_s(f_d + f_u)} = \frac{f_d^2 u_{sd}^2}{K_S(1-\delta)(1-\varepsilon_f)} \ldots\ldots\ldots\ldots\ldots\ldots\ldots \text{(38)}$$

Kunii et al, proposed the following expression for the vertical dispersion coefficient in terms of the measurable bubble and bed properties as

$$D_{sv} \cong \frac{f_w^2 \varepsilon_{mf} \delta d_b u_b^2}{3u_{mf}} \quad \ldots\ldots\ldots\ldots\ldots\ldots\ldots\ldots\ldots\ldots\ldots\ldots\ldots\ldots\ldots\ldots \text{(39)}$$

The horizontal movement of solids was first studied by Brotz [95] in a shallow rectangular bed from where he got the information to evaluate the horizontal dispersion coefficient $D_{Sh.}$. A similar approach was used by other investigators. Heertjes et

al. [96] suggested that the wake material scattered into the freeboard by the bursting bubbles could contribute significantly to the horizontal movement of solids of solid .Hirama et al. [97] and Shi and Gu [98] used partition plates in the freeboard just above the bed to a study this effect. All of these investigators used rather shallow beds of height between 5 and 35cm. In contrast, Bellgardt and Werther [99] made measurements in a much larger n bed, namely a 2m× 0.3m bed about 1m deep. Quartz sand (dp=450 μ m) was fluidized, and careful measurements confirmed that vertical mixing was much faster than the horizontal mixing, thus justifying the use oh a one dimensional dispersion model in the horizontal direction. Kunii and Levenspiel [94] developed a mechanistic model based on the Davidson bubble and proposed the following expression for the horizontal dispersion coefficient for both fast and intermediate bubbles.

$$D_{sh} = \frac{3}{16}\frac{\delta}{1-\delta}\alpha^2 d_b u_{br}\left[\left(\frac{u_{br}+2u_f}{u_{br}-u_f}\right)^{1/3} - 1\right] \quad \text{.....(40)}$$

For fast bubbles with thin clouds typical of fine particles system, or $u_{br} >> u_{f,}$ the above equation simplifies to

$$D_{sh} = \frac{3}{16}\frac{\delta}{1-\delta}\frac{\alpha^2}{\varepsilon_{mf}} u_{mf} d_b \quad \text{..... ..... (41)}$$

A number of binary mixtures (both homogeneous and heterogeneous) with different system parameters viz. particle size/density, initial static bed height, composition of the mixture, height of particle layers and superficial velocity of the fluidizing medium were studied exhaustively.

A theoretical model has been developed on the basis of 'counter flow solid circulation model' .Considering both vertical and horizontal movement of the jetsam particles as some particles displace horizontally due to the bursting of bubbles , the dispersion model in the form of the differential equation can be written as follows,

For upward motion i.e. in upward direction:

$$f_u D_{sv}\left(\frac{\partial^2 C_{ju}}{\partial z^2}\right)+ f_u u_u\left(\frac{\partial C_{ju}}{\partial z}\right)+ K_s\left(C_{ju}-C_{jd}\right)+ D_{sh}\frac{\partial^2 C_{ju}}{\partial z^2}=0 \ \ldots\ldots\ldots\ldots\ldots\ldots (42)$$

For down ward motion i.e. in downward direction:

$$f_d D_{sv}\left(\frac{\partial^2 C_{jd}}{\partial z^2}\right)+ f_d u_{jd}\frac{\partial C_{jd}}{\partial z}+ K_s\left(C_{jd}-C_{ju}\right)+ D_{sh}\frac{\partial^2 C_{jd}}{\partial z^2}=0 \ldots\ldots\ldots\ldots\ldots\ldots (43)$$

When superficial velocity of the fluidizing medium is more than the minimum fluidization velocity of the jetsam/flotsam particles, one stream having fraction moves up and the other stream with fraction moves down on the assumption that the whole solid materials is divided in two streams .Thus the movement of solids is a continuous process during fluidization. It is almost impossible to determine the exact fraction of solids moving up or down. Therefore, it has been assumed that half of the whole bed materials moves in upward direction while the other half moves in the downward direction during fluidization .Again with the assumption of $f_d = f_u$,$u_u = u_d$, $C_{ju} = C_{jd}$ and writing f ,u and C_j for these variables respectively in the above equation then adding these two equations the following equation is obtained,

$$2 fD_{sv}\left(\frac{\partial^2 C_j}{\partial z^2}\right)+ 2 fu_0\frac{\partial C_j}{\partial z}+ 2D_{sh}\frac{\partial^2 C_j}{\partial z^2}=0 \ldots\ldots\ldots\ldots\ldots\ldots\ldots\ldots\ldots\ldots (44)$$

Now substituting $(W/2\rho_S)/V_b$ for f, the above equation can be written as follows,

$$\left(\frac{WD_{sv}}{V_b\rho_s}+2D_{sh}\right)+\frac{\partial^2 C_j}{\partial z^2}+\frac{Wu_0}{V_b\rho_s}\frac{\partial C_j}{\partial z}=0 \ldots\ldots\ldots\ldots\ldots\ldots\ldots\ldots\ldots\ldots (45)$$

It can be further written as

$$\frac{\partial^2 C_j}{\partial z^2}+\frac{Wu_0}{WD_{sv}+2D_{sh}\rho_s V_b}\frac{\partial C_j}{\partial z}=0 \ldots\ldots\ldots\ldots\ldots\ldots\ldots\ldots\ldots\ldots (46)$$

This is the differential equation describing the concentration of jetsam as a function of bed height. Vertical mixing rate in rather small beds as given

$D_{sv} = 0.06 + 0.1u_0$ …… (47)

Horizontal dispersion coefficient as described by Kunii and Levenspiel and has been simplified using the following expression

$$\delta = \frac{u_0 - u_{mf}}{u_b + u_{mf}}$$

$$u_f = \frac{u_{mf}}{\varepsilon_{mf}}$$

$$u_b = 1.6 * \left\{ \left[\left(u_0 - u_{mf} \right) + 1.13 * d_b^{0.5} \right] * d_t^{1.35} + u_{br} \right\}$$

$$u_{br} = 0.711 * \sqrt{g d_b}$$

$$d_b = 0.853 * \left[1 + 0.272 \left(u_0 - u_{mf} \right) \right]^{1/3} * \left(1 + 0.0684 z \right)^{1.21}$$

The simplified form of D_{sh} is

$$D_{sh} = \frac{3}{16} \times \frac{u_0 - u_{mf}}{u_b - u_0 + 2u_{mf}} \times \frac{\alpha^2 \times u_{mf} \times \left(d_b / 100 \right)}{\varepsilon_{mf}} \text{ …….. (48)}$$

$$= K^{'} \times \frac{K_1 \left(1 + 0.0684 Z \right)^{1.21}}{C_1 + D_1 d_b^{1/2}} = K^{'} \times \frac{K_1 \left(1 + 0.0684 Z \right)^{1.21}}{C_1 + D_2 \left(1 + 0.0684 Z \right)^{0.605}}$$

Expanding the above two series as per Tayler series D_{sh} can be written as

$$D_{sh} = \frac{K^{'} \times K_1 \left(1 + 0.0828 Z \right)}{C_1 + D_2 \left(1 + 0.0414 Z \right)} K_1$$

Where,

$$K^{'} = \frac{3}{1600} \times \frac{u_{mf}\left(u_0 - u_{mf}\right)}{\varepsilon_{mf}} \alpha^2$$

$$K_1 = 0.853 * \left[1 + 27.2\left(u - u_{mf}\right)\right]^{1/3}$$

$$C_1 = 1.6\, d_t^{1.35}\left(u_0 - u_{mf}\right) - u_0 + 2u_{mf}$$

$$D_1 = 1.808\, d_t^{1.35} + 0.711 g^{1/5}$$

$$D_2 = D_1 * K_1^{1/2}$$

Equation 46 can be written as

$$\frac{\partial^2 C_j}{\partial z^2} + \frac{F u_0}{F D_{sv} + D_{sh}} \frac{\partial C_j}{\partial z} = 0 \text{ ……………………………… (49)}$$

Where $F = \frac{W}{2\rho_s V_b}$

Now describing the coefficient of $\frac{\partial C_J}{\partial Z}$ as a function of height as

$$\frac{F u_0}{F D_{sv} + D_{sh}} = f(z) \text{ …………………………………… (50)}$$

The equation no. 49 can be written as,

$$\frac{\partial^2 C_j}{\partial z^2} + f(z)\frac{\partial C_j}{\partial z} = 0 \text{ …………………………………….. (51)}$$

Solving the above differential equation by variable separable, method the concentration of jetsam particles can be written as,

$$C_j = \int e^{-\int f(z)dz} dz \text{ …………………………………. (52)}$$

Now substituting the D_{sh} and D_{sv} the following expression has been obtained

$$f(z) = \frac{A + Bz}{C + Dz} \quad \text{..... (53)}$$

Where,

$A = Fu_0C_1 + Fu_0D_2$

$B = 0.0414 \times Fu_0D_2$

$C = (0.06 + 0.1u_0)FD_2 + KK$

$D = (0.06 + 0.1u_0) \times 0.00414 \times FD_2 + 0.0828 \times KK_1$ Now the solution of the above the

$$C_j = \int e^{-(B/D)z} \times \left(1 + \frac{D}{C}\right)^{\frac{BC-AD}{D^2}} dz$$

Solution of differential equation in terms of A, B, C, and D.

Again on simplification above equation can be written as,

$$C_j = -\frac{D}{B}e^{-\left(\frac{B}{D}\right)z} - \left(\frac{BC - AD}{BC}\right)e^{-\left(\frac{B}{D}\right)z}Z - \frac{(BC - AD)}{CD} \times \frac{D^2}{B^2}e^{-\left(\frac{B}{D}\right)z} \quad \text{..... (54)}$$

This gives the expression for the concentration of jetsam particles for any system at any height of the bed from the distributor [02] .Thus finally the mixing index at nay height can be written as

$$I_M = C_j \times \frac{W}{J} \quad \text{.....(55)}$$

3.4.1 Solution of the differential equation by finite difference method

For upward motion i.e. in upward direction:

$$f_u D_{sv}\left(\frac{\partial^2 C_{ju}}{\partial z^2}\right) + f_u u_u\left(\frac{\partial C_{ju}}{\partial z}\right) + K_s\left(C_{ju} - C_{jd}\right) + D_{sh}\frac{\partial^2 C_{ju}}{\partial z^2} = 0 \quad \text{..... (42)}$$

$$\left[f_u D_{sv} + D_{sh}\right]\frac{\partial C_{ju}^{\ 2}}{\partial z^2} + f_u u_{ju}\frac{\partial C_{ju}}{\partial z} + K\left(2C_{ju} - 1\right) = 0 \quad \text{..... (42)(a)}$$

Since $C_{ju} + C_{jd} = 1$

Taylor series

$y(x+h) = y(x) + hy'(x) + \frac{h^2}{2} y''(x) + \frac{h^3}{6} y'''(x) + \ldots\ldots\ldots\ldots\ldots\ldots$ (56)

$\Rightarrow y'(x) = \frac{y(x+h) - y(x)}{h} - \frac{h}{2} y''(x) -$

$\Rightarrow y'(x) = \frac{y(x+h) - y(x)}{h} + o(h)$ …… (57)

Similarly

$y(x-h) = y(x) - hy'(x) + \frac{h^2}{2} y''(x) - \frac{h^3}{6} y'''(x) + \ldots\ldots\ldots\ldots\ldots\ldots$ (58).

$\Rightarrow y'(x) = \frac{y(x) - y(x-h)}{h} + o(h)$ …….. (59)

A central difference approximation for y'(x) can be obtained by subtracting equation C from equation A, so we have

$y'(x) = \frac{y(x+h) - y(x-h)}{2h} + oh^2$ ……..(60).

If we add the equation C and A, we will get

$y''(x) = \frac{y(x-h) - 2y(x) + y(x+h)}{h^2} + o(h^2)$ ……..(61)

Putting Cju = y_i in equation 2 and taking $x_i = x_0 + ih, i = 1,2,\ldots\ldots,n$

The corresponding values of y at these points are denoted by

$y(x_i) = y_i = y(x_0 + ih), i = 0,1,2,\ldots\ldots n$

Equation (42) (a) becomes

$[f_u D_{SV} + D_{sh}]y_i'' + f_u u_{ju} y_i' + K(2y_i - 1) = 0$ …… (62)

Putting y_i' and y_i'' value from equation E and F in above equation we will get

$$\left[f_u D_{sv} + D_{sh}\right]\left[\frac{y_{i-1} - 2y_i + y_{i+1}}{h^2}\right] + f_u u_{ju}\left[\frac{y_{i+1} - y_{i-1}}{2h}\right] + K(2y_i - 1) = 0 \text{ ..... (63)}$$

Let

$$f_u D_{sv} + D_{sh} = A$$

$$f_u u_{ju} = B$$

$$\text{A}\left[\frac{y_{i-1} - 2y_i + y_{i+1}}{h^2}\right] + B\left[\frac{y_{i+1} - y_{i-1}}{2h}\right] + 2Ky_i = K \text{ ..... (64).}$$

Multiplying both the side by h^2 we get

$$A\left[y_{i-1} - 2y_i + y_{i+1}\right] + BH\left[\frac{y_{i+1} - y_{i-1}}{2}\right] + 2Kh^2 y_i = Kh^2$$

$$\Rightarrow \left[A - \frac{Bh}{2}\right]y_{i-1} + \left[2Kh^2 - 2A\right]y_i + \left[A + \frac{Bh}{2}\right]y_{i+1} = Kh^2 \text{ ..... (65)}$$

n equal sub interval of width h

nh = 24

$\Rightarrow n \times 2 = 24$

$\Rightarrow n = 12$

Putting h=2 in last equation, it becomes

$$\left[A - B\right]y_{i-1} + \left[8K - 2A\right]y_i + \left[A + B\right]y_{i+1} = 4K \quad \text{.....(66)}$$

Putting i=1, 2, 3…. Up to 11 in above equation, corresponding equations are

$$[A-B]y_0+[8K-2A]y_1+[A+B]y_2=4K$$
$$[A-B]y_1+[8K-2A]y_2+[A+B]y_3=4K$$
$$[A-B]y_2+[8K-2A]y_3+[A+B]y_4=4K$$
$$[A-B]y_3+[8K-2A]y_4+[A+B]y_5=4K$$
$$[A-B]y_4+[8K-2A]y_5+[A+B]y_6=4K$$
$$[A-B]y_5+[8K-2A]y_6+[A+B]y_7=4K$$
$$[A-B]y_6+[8K-2A]y_7+[A+B]y_8=4K$$
$$[A-B]y_7+[8K-2A]y_8+[A+B]y_9=4K$$
$$[A-B]y_8+[8K-2A]y_9+[A+B]y_{10}=4K$$
$$[A-B]y_9+[8K-2A]y_{10}+[A+B]y_{11}=4K$$
$$[A-B]y_{10}+[8K-2A]y_{11}+[A+B]y_{12}=4K$$

Taking

$a_1=a_2=a_3=....=a_{11}=A-B$

$b_1=b_2=b_3=.....=b_{11}=8K-2A$

$c_1=c_2=c_3=.....=c_{11}=A+B$

$d_1=d_2=d_3=.....=d_{11}=4K$

$y_1, y_2, ... y_{12}$ values can be found by using formula

(1) Taking $\alpha_1=b_1$

Then $\alpha_i=b_i-\frac{a_i c_{i-1}}{\alpha_{i-1}}$, i= 2,3,……n ……. (67)

(2) Taking $\beta_1=\frac{d_1}{b_1}$

Then $\beta_i=\frac{d_i-a_i\beta_{i-1}}{\alpha_i}$, i = 2, 3, …n …….. (68)

(3) Taking $y_n=\beta_n$

Then $y_i = \beta_i - \frac{c_i y_{i+1}}{\alpha_i}$, i = n-1, n-2,…….1 …….. (69)

(Ref 100)

$$D_{sv} = 0.06 + 0.1u_0$$

$$D_{sh} = \frac{3}{16} \times \frac{u_0 - u_{mf}}{u_b - u_0 + 2u_{mf}} \times \frac{\alpha^2 \times u_{mf} \times (d_b / 100)}{\varepsilon_{mf}} \ldots\ldots$$

$$= K' \times \frac{K_1 (1 + 0.0684Z)^{1.21}}{C_1 + D_1 d_b^{1/2}} = K' \times \frac{K_1 (1 + 0.0684Z)^{1.21}}{C_1 + D_2 (1 + 0.0684Z)^{0.605}}$$

Expanding the above two series as per Tayler series D_{sh} can be written as

$$D_{sh} = \frac{K' \times K_1 (1 + 0.0828Z)}{C_1 + D_2 (1 + 0.0414Z)} K_1$$

Where,

$$K' = \frac{3}{1600} \times \frac{u_{mf} (u_0 - u_{mf})}{\varepsilon_{mf}} \alpha^2$$

$$K_1 = 0.853 * \left[1 + 27.2(u - u_{mf})\right]^{1/3}$$

$$C_1 = 1.6 d_t^{1.35} (u_0 - u_{mf}) - u_0 + 2u_{mf}$$

$$D_1 = 1.808 d_t^{1.35} + 0.711 g^{1/5}$$

$$D_2 = D_1 * K_1^{1/2}$$

$$f_u D_{sv} + D_{sh} = A$$

$$f_u u_{ju} = B$$

a = A-B

b = 8K-2A

c = A+B

α = 0.77

We have taken K11 instead of K' and t instead of α

Chapter 4

EXPERIMENTAL ASPECTS

CHAPTER-4

EXPERIMENTAL ASPECTS

4.1 Experimental Set Up

The experimental set up primarily consists of the following major components

1. Air Compressor
2. Air accumulator
3. Pressure gauge
4. Rotameter
5. Air distributor
6. Calming section
7. Fluidizer
8. Manometer
9. Promoters
10. Control Valve
11. Vacuum Pump

Sago is taken as bed material whose density is1304 kg/ m^3 .The column inside diameter is 14 cm. The experimental set up is given in figure-5(Appendix 1).

4.2 Experimental Procedure

4.2.1 Static bed condition:

After fluidizing the bed with a particular fluid mass velocity, it was brought to static condition by closing the air supply. The bed was then divided into different layers each of two cm height. Each of the layers was drawn applying suction and analyzed for the amount of jetsam particles present. Such a system was referred as the static bed condition.

4.2.2 Fluidized Bed Condition:

The bed was fluidized at a fixed fluid mass velocity and under steady state condition; the samples of the materials were drawn through the side ports of the column which are located at intervals of two cm along the column height on the either side alternately. The samples drawn in such a manner were analyzed for the amount of jetsam particles. This system was referred to as the fluidized bed condition.

The data for different systems with different system parameters were observed through the following types of bed dynamics

(a) Static bed condition
(b) Unprompted fluidized bed condition
(c) Promoted fluidized bed condition(using a rod- promoter)
(d) Promoted fluidized bed condition(using a disc- promoter)

The experimental data for the jetsam concentration art different heights of the bed for homogeneous systems have been observed with various initial static bed height, fluidization velocity of the mixture and height of particles layers. These data have been processed to predict the mixing index by developed mathematical model.

After solving the differential equation, a C- program was written for developing the model. The program was tried for different type of bed conditions by varying fraction of bed materials, jetsam velocity, and minimum fluidization velocity of mixtures. Fraction of bed material was varied from 0 to 1 and minimum fluidization velocity was varied from minimum fluidization velocity of smaller size particles, 0.465m/s to that of bigger size particles, 1.0335 m/s.

Chapter 5

RESULT AND DISCUSSION

CHAPTER 5
RESULT AND DISCUSSION

A theoretical model has been developed on the basis of 'counter flow solid circulation model'. Considering both vertical and horizontal movement of the jetsam particles as some particles displace horizontally due to the bursting of bubbles, the dispersion model in the form of the differential equation can be written as follows,

For upward motion of jetsam particles i.e. in upward direction:

$$f_u D_{sv}\left(\frac{\partial^2 C_{ju}}{\partial z^2}\right) + f_u u_u\left(\frac{\partial C_{ju}}{\partial z}\right) + K_s\left(C_{ju} - C_{jd}\right) + D_{sh}\frac{\partial^2 C_{ju}}{\partial z^2} = 0.$$

The above differential equation is solved by finite difference method and finally solved by the formula given below :

(1) Taking $\alpha_1 = b_1$

Then $\alpha_i = b_i - \frac{a_i c_{i-1}}{\alpha_{i-1}}$, i= 2,3,……n

(2) Taking $\beta_1 = \frac{d_1}{b_1}$

Then $\beta_i = \frac{d_i - a_i \beta_{i-1}}{\alpha_i}$, i = 2, 3, …n

(3) Taking $y_n = \beta_n$

Then $y_i = \beta_i - \frac{c_i y_{i+1}}{\alpha_i}$, i = n-1, n-2,…….1

where

$a_1 = a_2 = a_3 = ... = a_{11} = A - B$

$b_1 = b_2 = b_3 = ... = b_{11} = 8K - 2A$

$c_1 = c_2 = c_3 = ... = c_{11} = A + B$

$d_1 = d_2 = d_3 = ... = d_{11} = 4K$

$f_u D_{sv} + D_{sh} = A$

and $f_u u_{ju} = B$

The results are obtained by trying the program for different types of bed conditions with varying fraction of bed materials, jetsam velocity, and minimum fluidization velocity of mixtures. Fraction of bed material was varied from 0 to 1 and minimum fluidization velocity was varied from minimum fluidization velocity of smaller size particles, 0.465m/s to that of bigger size particles, 1.0335 m/s. These results obtained are given in tables 2.1 to 2.7 (**Appendix-3**). The results obtained from theoretical model are compared with experimental values. Then percentages of error are obtained from the comparison of two values are given in tables 2.1 to 2.7(**Appendix-3).** Mixing index with the above mentioned conditions are calculated with different static bed heights (24cm, 20cm, 16cm, 12cm), with different minimum fluidization velocities (0.862m/s,1.027m/s,1.234m/s) and with different jetsam particle compositions (25:75, 40:60, 50:50, 90:10). Samples of these calculations are given in tables- 3.1, 3.2 and 3.3 **(Appendix-4).**

Graphs are plotted between mixing index and bed height with different static bed height, different fluidization velocity, and different jetsam particles composition and with different fractions of bed material **(Figure -5.1, 5.2, 5.3 and 5.4).** There is also a graph plotted to know the difference between mixing index in promoted and unpromoted fluidized bed **(Figure-5.5).** In all the above cases mixing index is taken as dependent variable and bed height is as independent variable.

It is observed that mixing index decreases as bed height increases. Mixing Index sharply decreases from bed height 0 to 5 cm but then it changes a little between bed height 5cm to 15cm .As static bed height increases, corresponding Mixing Index values decreases **(Fig- 5.1 and Table-3.1).** It is due to fact that for a greater bed height, a greater fluidization velocity is needed to fluidize the bed. So for a greater bed height and for corresponding greater fluidization air velocity ,more jetsam particles goes upward comparing to lower bed height.

It is observed that as operating fluidization increases, corresponding mixing index values decreases **(Fig- 5.3 and Table-3.2)**. It is due to reason that as fluidization velocity increases, concentration of jetsam particles decreases because they go

upward. Since mixing index directly proportional to concentration jetsam particles, lower values of mixing index will get from a higher fluidization velocity.

From results obtained it is observed that when jetsam particle composition in mixture increases, mixing index values decreases **(Fig- 5.2, Table-3.3)**. It is due to reason that mixing index is inversely proportional to weight of jetsam.

It is also observed that as fractional values of bed material increases, higher mixing index will get. But it does not go for higher fraction as shown in graph **(Fig-5.4,Table-3.4)**.When fractional values reaches to 20% mixing index values does not obey any order .So a optimum fraction of bed material with respect to its distribution in upward and the downward streams during fluidization process is taken

It is found that unpromoted fluidized bed gives higher mixing index in maximum cases indicating better mixing than promoted beds. This implies that better mixing is obtained with unpromoted bed for its greater available of flow area **(Fig- 5.5 and Table-3.5).** Mixing index of disc promoted and rod promoted fluidized bed is almost same **(Appendix-3).**

It is also found that mixing index by theoretical model is lower than the experimental one for maximum cases **(Appendix-3)**. It is due to gulf streaming effect during fluidization .But some times experimental mixing index values less than theoretical mixing index **(Table-2.2.3, 2.2.6, 2.3.6, 2.4.5, 2.5.4, 2.5.5 and 2.7.6)**.It is due to the reason that presence of promoter, gulf streaming effect is less.

It is observed that the percentage of error in case of static bed height condition in all type of cases is more **(Table 2.1.1, 2.2.1, 2.3.1, 2.4.1, 2.5.1, 2.6.1 and 2.7.1).** In these cases, the operating fluidization velocity is nearly equal or higher then the bigger size particles minimum fluidization velocity (1.0335 m/s) .So there is a good mixing between jetsam and flotsam particles. In the fluidized bed which later becomes to static bed .The other reason is that in fluidized bed condition where particle distribution is in continuous and dispersed phases are different to affect the ultimate mixing phenomena. Gulf streaming effect is also there.

The reason for high experimental value for fluidized condition, the samples were drawn from the ports made on either side of the column alternatively and analyzed on the basis of assumption of uniform concentration for a particular layer of particles across the cross section of the column at any height.

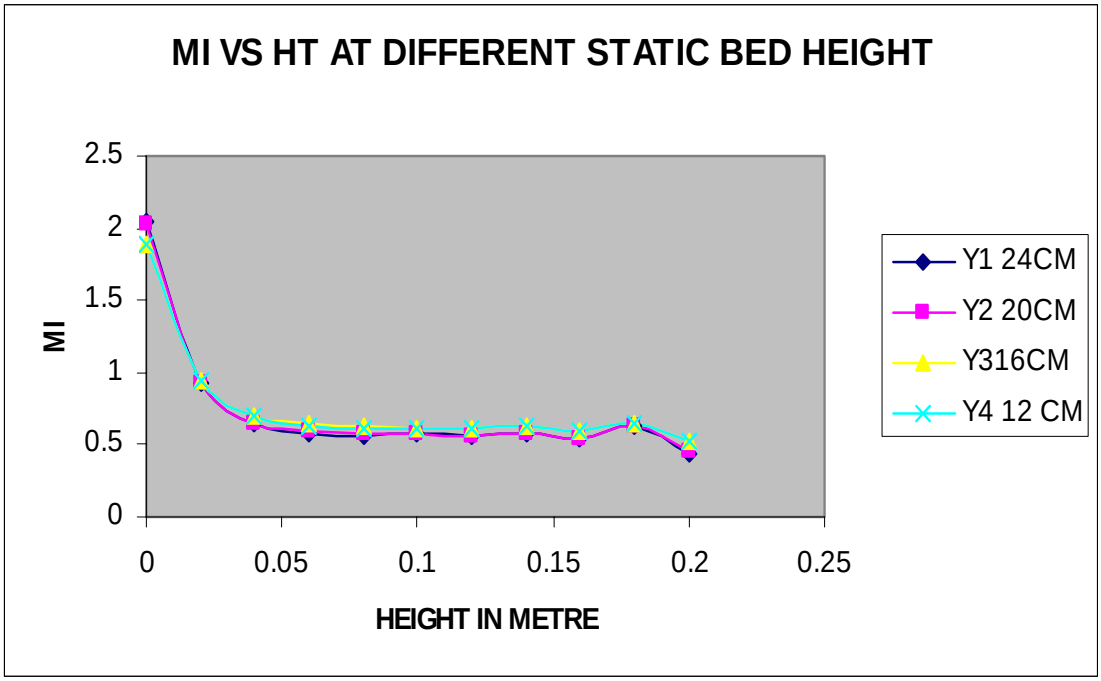

Figure-5.1 Mixing index vs bed height at different static bed height

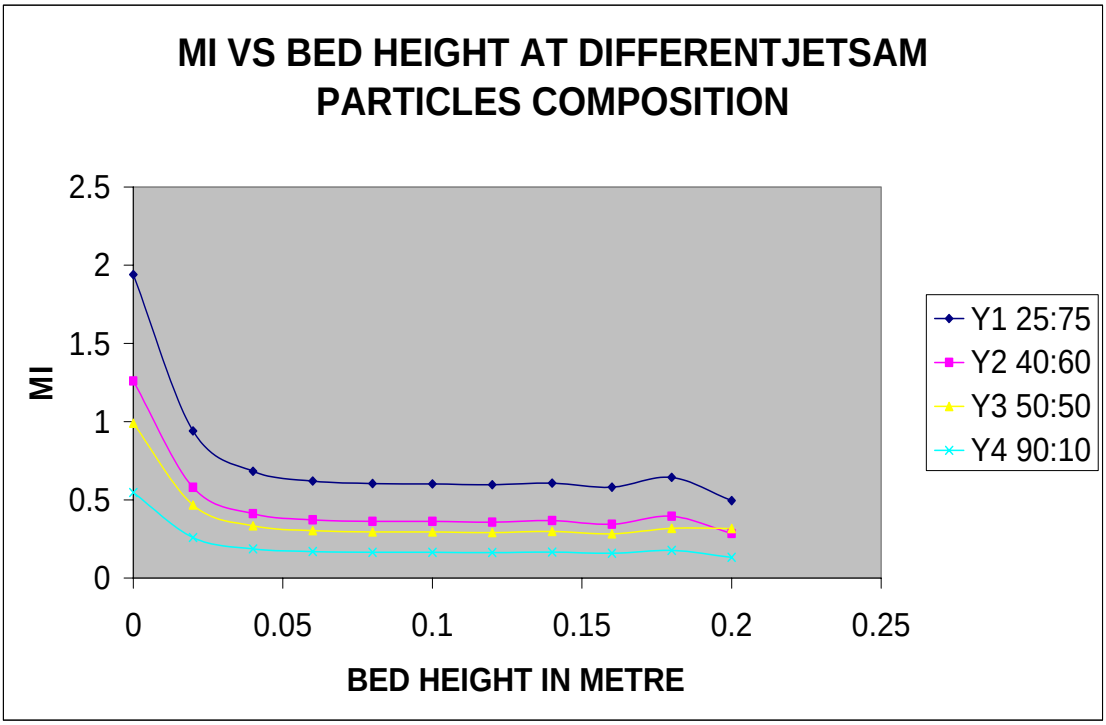

Fig-5.2 Mixing index vs bed height at different jetsam particles composition

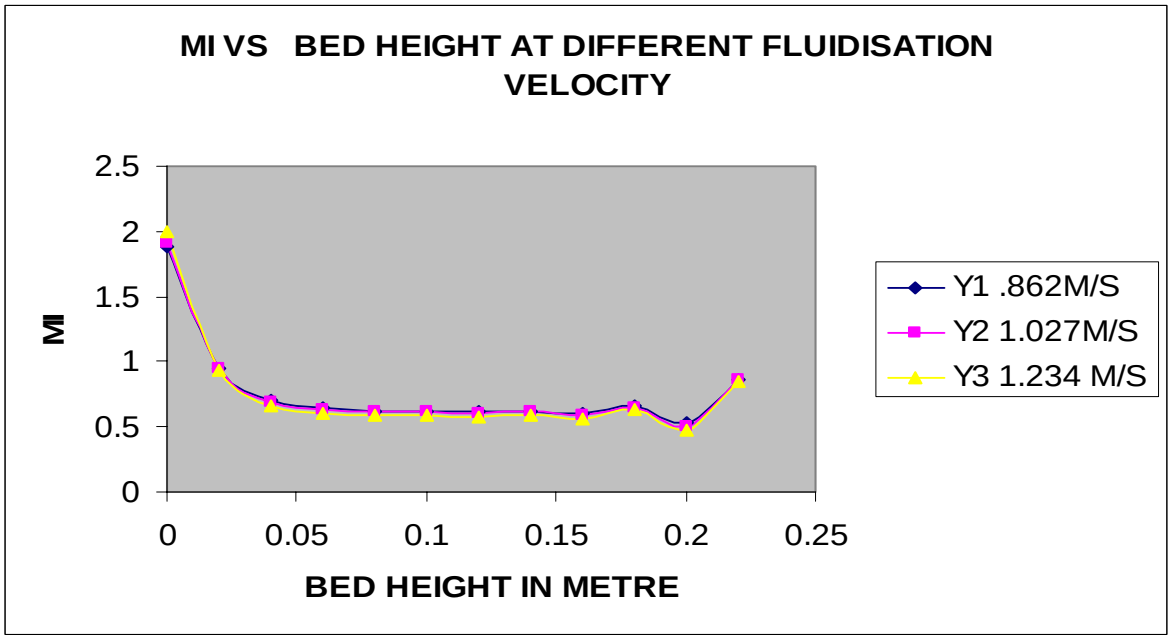

Figure-5.3 Mixing index vs bed height at different fluidization velocity

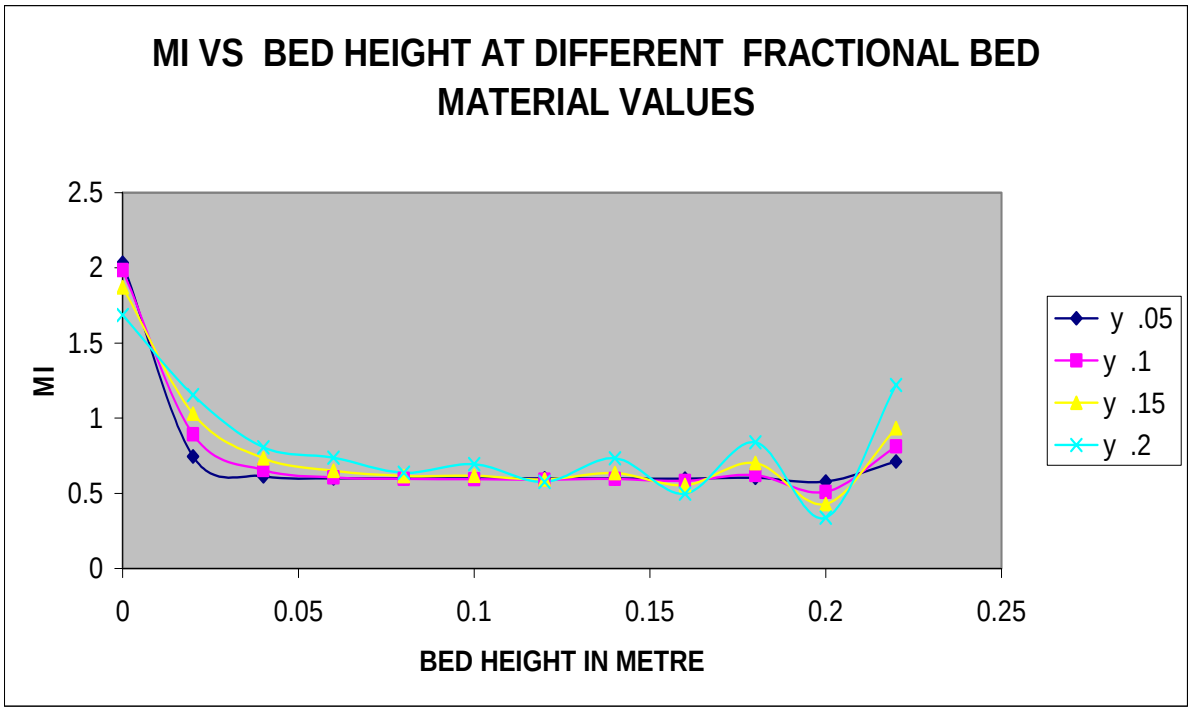

Figure-5.4 Mixing index vs bed height at different fractional bed material values

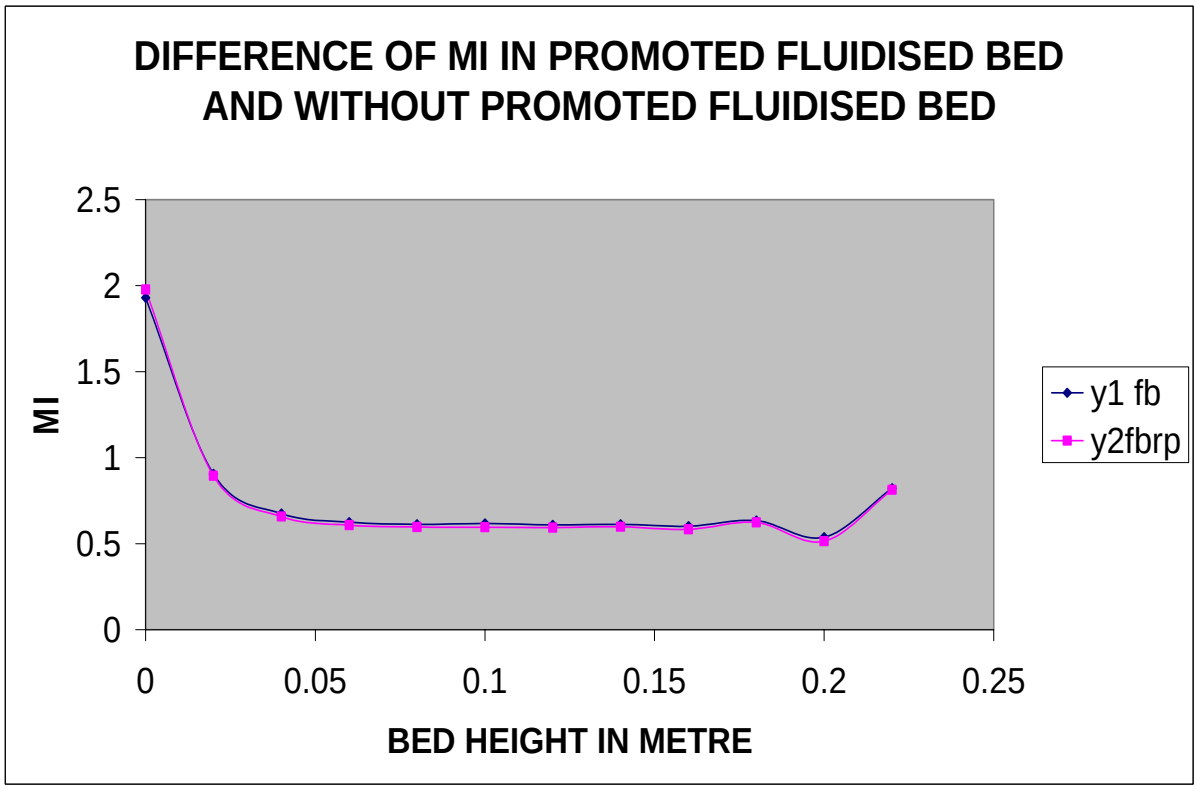

Figure-5.5 Mixing index vs bed height in promoted and unpromoted fluidized bed

Chapter 6

CONCLUSION

CHAPTER-6

CONCLUSION

A model of solid mixing in a gas-solid fluidized bed has been developed and tested existing experimental data. The finite difference method is used to solve the differential equation. The numerical results are in satisfactory agreement with experimental data. In the way of the developing the model fraction of bed material, jetsam particles velocity, minimum fluidization velocity of the mixture are taken as variable. It is observed that both the concentration of the jetsam particles and mixing index decreases with the height of particles layers in the bed (measured from the distributor).It is also observed that the unpromoted bed gives better mixing index values than promoted bed due to its greater flow area. Optimum fraction of bed materials with respect to its distribution in the upward and downward streams during the fluidization process can be taken up to 20%.When static bed height, operating fluidization velocity and jetsam particles composition values increases, for all the cases corresponding mixing index values decreases. It is seen that mixing index values of disc promoted bed and rod promoted fluidized bed are nearly same although flow area of rod promoted fluidized bed is greater than disc promoted fluidized bed.

Future work:

Further work can be carried out for irregular particles such as dolomite, coal, sand, iron etc. Flotsam and jetsam particles density is an important parameter. Therefore density of particles may be taken into consideration while developing the model. Rectangular or conical fluidized bed can also be considered in place of cylindrical bed.

NOMENCLATURE

Cj : Concentration of jetsam particles at any height in the bed (amount of jetsam particles in the sample drawn at a height in kg/ amount of that in the original mixture in kg

d : Diameter of bed ,m

$\bar{d}_p$: Average particle size of the mixture, m

Dc : Diameter of the column,m

D_E : Equivalent diameter of the column,m

D_{sh} : Horizontal dispersion coefficient, m^2 / s

D_{sv} : Vertical dispersion coefficient, m^2 / s

f :Fraction of solids moving up or down per bed volume, m^3 of the solid / m^3 of the bed volume

Hb : Height of the particles layer in the bed from distributor,m

Hs : Initial static bed height,m

I_M : Mixing Index, dimensionless

J : W eight of jetsam particles taken in the bed,kg

K : Coefficient of correlation

Ks : Interchange coefficient

k,n : Exponent for variables

M : Equilibrium mixing index

u : Velocity of the stream of particles moving up or down,m/s

uf : Rise velocity of the emulsion gas m/s

U : Superficial velocity of the fluidizing medium

Uf : Minimum fluidization velocity of the flotsam particles, m/s

U_{T0} : Take over velocity defined as the value of U corresponding toM=0.5

V_b : Volume of the bed, m^3

W : Weight of the total bed material, kg

X^* : Percentage of jetsam particle in any layer

$\overline{X}_{bed}$: Percentage of jetsam particle in the bed

Z : Height of particles layer in the bed from the distributor, varying from 0 to 0.2 m

d_j : Diameter of the bigger particles, μ m

d_f : Diameter of the smaller particles, μ m

A : Part of the horizontal section of the riser, occupied by ascending particles (core zone)

B : Part of the horizontal section of the riser, occupied by descending particles (annularZone)

Frt : Froude number,

u : superficial gas velocity, m/s

ut :single-particle terminal velocity, m/s

u1, u2 : axial velocities of particles in the core zone and the annular zone, m/s

$\rho = A\rho_1 + B\rho_2$,density of the bed mean over horizontal section of the riser,kg/ m^3

ρ_1, ρ_2 : Density of the bed in the core and annular zone in kg/ m^3

H : Height of the riser,m

Ho : Height of the bottom of the fluidized bed,m

J_s : Mass circulating flow of particles, $kg/m^2 s$

$\bar{J}_s$: Dimension less mass flow of particles

β_* : Coefficient of interphase exchange 1/s

β_1 : Coefficient ,1/s

t : Time,s

τ : Continum phase viscous stress tensor, kg/ms^2

ϖ : Rotational velocity

C_1 : Concentration in core zone

C_2 : Concentration in annular zone

D_a, D_r : Coefficient of axial and radial dispersion of particles, m^2/s

V_s : Velocity of particles,m/s

x :Vertical co-ordinate,m

f : Volumetric fraction of a phase(m^3/m^3)

Q_1 : Feeding rate of particles per thickness at the position(x,y) (kg/m.s)

Q_2 : Drainage rate of particles per thickness at the position(x,y)(kg/m.s)

K_w : Wake exchange coefficient

δ : Volumetric fraction of bubbles in the bed, m^3 of bubble/ m^3 of bed

A_C : Area of the fluidizer, m^2

h : Bed height above distributor level,m

h_{mf} : Bed height above distributor level,m at minimum fluidization

ho :A measure of the initial bubble size,m

K_{mb} : Constant for minimum bubbling velocity

n : Number of orifices in distributor plate

Xi : Weight fraction of particles of diameter d_s

U_{mb} : Minimum bubbling velocity,m/s

Suffixes:

b : bubble

br : bubble rise

f : fluidizing condition

j : jetsam

m : mixture

mf : minimum fluidization condition

u : upward component

d : downward component

o : operating condition

s : solids

t : column

w : wake solids

E : Emulsion

Greek Words

α : ratio of equivalent diameter of wake fraction of bubble diameter

ε : bed voidage fraction

δ : Volumetric fraction of bubbles

ρ : density of particles,kg/m^3

REFERENCES

1. B.V.Babu, “process plant simulation”, Oxford University press, New Delhi, ndia(2004)
2. A Ph.D Thesis by Asst. Prof Dr (Mrs.) Abanti Sahoo “Mixing and segregation characteristics of binary mixtures of irregular particles in promoted gas-solid fluidized bed”.
3 Wu, S.Y and Baeyens, J. Powder Technology, 98(1998)139
4 J.W.Carson,T.A.Royal,D.J. Goodwill,Bulk solids handling,6,1,Feb(1986),139
5 M.A..Gilbertson and I.Eames;Jurnal of fluid mechanics;433,(2001),347
6. Nienow, A.W.,Cheesman,D.J. in J.R.Grace,J.M.Matsen(eds)Fluidisation plenum,New-York,(1980),373.
7. T.Chiba,Fluidisation,Second edition,Academic press(1985),9.
8. Chiba,S., Nienow, A.W.,T.Chiba, Powder Technology,26,(1980),1~10
9. N.S.Naimer,T.Chiba and Nienow, A.W.:Chemical Engineering science 37,7,(1982),1047
10. P.N. Rowe,A.W.Nienow and A. J. Agbim:Transaction of Institution of Chemical Engineers,50,(1972),310,324
11. Fan,L.T.,Chang,Y.,The Canadian journal of chemical engg.57 Feb (1979)
12. Hoffman,A.C.(download from internet) Manipulating fluidized bed using internals:Fluidisation with baffles, NPT Proscestechnologie,7 No.2(2000)20-24
13. Hartholt,G.P.Riviere,la R., Hoffman,A.C. And Jansen,L.P.B.M., Powder Technology,93(1997),185-188
14. Rowe,P.N.,Partridge,B.A.,Cheney,A.G.,Henwood,G.A andLyali,A.,Trans. instn. chem.enges.,43,(1965)
15. Richardson and Zaki, Transaction of Institution of Chemical Engineers, 32(1954), 35
16. Peeler,J.P.;Huang, J.R.;Chemical Engineering science,44(5),(1989),1113
17. N.S.Naimer,T.Chiba and Nienow, A.W,Chemicalengg. Communication, 62(1987),53
18. Formisani,B., Powder Technology,66,(1991),259
19. Wen,Y.C. and Yu, Y.H., Chemical Engineering progress symposium series, 62,(1966),100
20. I.N.M. Wooland and O.B.Potter AIChE Journal, 14,3,may(1968)
21 Gibilaro,L.G. and Rowe ,P.N.: Chemical Engineering science,29,(1974) 1403
22. Feng, Y.Q., Yu, A.B., 2004. An assessment of model formulations in discrete Particle simulation of gas solid flow. I&EC Research 43, 8378-8390.

23 Nienow, A.W., Chiba, T., 1981. Solid mixing and segregation in gas-fluidized Beds. The Institution of Chemical Engineers Symposium Series, vol. 65. Mixing of Particulate Solids, pp. S2/F/1-S2/F-19

24 Marzocchella, A., Salatino, P., Di Pastena, V., Lirer, L., 2000. Transient fluidization and segregation of binary mixtures of particles. A.I.Ch.E Journal 46, 2175–2182

25 R.J.Wakeman and B.W.Stopp: Powder Technology,13(1976)361

26 A.W. Nienow,P.N.Rowe and Cheung,L., powder technology,20(1978)89

27 Fan,L.T.,Chen,Y. and Lai,F.S., powder technology,61(1990)255

28 J. Kawabata,Y. Tajaki,T.Chiba,K.Yoshida: Journal of Chemical Engineering of Japan,14,3,(1981)

29 Nicholson, W.J. and Smith, J.C., Chemical Engineering progress 62, 83(1966)

30 A.P. Baskakov, in: V.G. Ainshtein, A.P. Baskakov (Eds.), Fluidization, Khimiya, Moscow, pp. 333–395

31 Yu.S. Teplitskii, V.A. Borodulya, E.F. Nogotov, Axial solids in a circulating fluidized Bed Int. J. Heat Mass Transfer 46 (2003) 4335– 4343

32 F.Wei, Z. Wang, Y. Jin, et al., Dispersion of lateral and axial solids in a cocurrent down Flow circulating fluidized bed, Powder Technol. 81 (1994) 25–30

33 G.S. Patience, J. Chaouki, Solids hydrodynamics in the fully developed region of CFB risers, in : Proceedings of the Eighth Engineering Foundational Conference on Fluidization, Tours, 1995, vol. 1, pp. 33– 40.

34 Yu.S. Teplitskii, Near-wall hydrodynamics of a circulating fluidized bed, Inzh.-Fiz. Zh. 74 (5) (2001) 177–181

35 V..A. Borodulya, Yu.S. Teplitskii, Scale transition in the circulating bed, in:proceedings of Minsk International Forum ‘‘Heat and Mass Transfer – MIF-96,’’ Minsk, 20–24 May 1996, vol. 5, pp. 69–74.

36 Y.S. Teplitskii, V.I. Kovenskii, Resistance of a circulating Fluidized bed, Inzh.- Fiz. Zh. 74 (1) (2001) 62–66.

37 Yu.S. Teplitskii, Setting of a boundary-value problems of longitudinal solids mixing in circulating Fluidizedbeds, Inzh.-Fiz. Zh. 76 (1) (2001) 80–83

38 B. Bader, J. Findlay, T.M. Knowlton, Gas/solids flow patterns in a 30.5-cm-diameter irculating fluidized bed, in: P. Basu, J.F. Large (Eds.), Circulating Fluidized Bed technology, Compeigne, 1988, pp.123–128

39 Feng, Y.Q., Pinson, D., Yu, A.B., Chew, S.J., Zulli, P., 2003. Numerical study of

Gas–solid .ow in the raceway of a blast furnace. Steel Research International 74, 523–530.

40 Tsuji, Y., Kawaguchi, T., Tanaka, T., 1993. Discrete particle simulation of two-dimensional .uidized bed. Powder Technology 79–87.

41 Hoomans, B.P.B., Kuipers, J.A.M., Van Swaaij, W.P.M., 2000. Granular dynamics simulation of segregation phenomena in bubbling gas-fluidized beds. Powder Technology 109, 41–48.

42 Xu, B.H., Yu, A.B., 1997. Numerical simulation of the gas–solid flow in a fluidized. bed by combining discrete particle method with computational fluid dynamics. Chemical Engineering Science 52, 2786–2809

43 Mikami, T., Kamiya, H., Horio, M., 1998. Numerical simulation of cohesive powder behavior in a fluidized bed. Chemical Engineering Science 53, 1927–1940.

44 Tsuji, Y., Kawaguchi, T., Tanaka, T., 1993. Discrete particle simulation of two-dimensional Fluidized bed. Powder Technology 79–87.

45 Ouyang, J., Li, J., 1999. Discrete simulation of heterogeneous structure and dynamic behavior in gas–solid fluidization. Chemical Engineering Science 54, 5427–5440.

46 Rong, D.G., Mikami, T., Horio, M., 1999. Particle and bubble movements around tubes immersed in fluidized beds—a numerical study. Chemical Engineering Science 54, 5737–5754

47 Xu, B.H., Yu, A.B., Chew, S.J., Zulli, P., 2000. Simulation of the gas–solid flow in a in a bed with lateral gas blasting. Powder Technology 109, 14–27.

48 Yuu, S., Umekage, T., Johno,Y., 2000. Numerical simulation of air and particle motions in bubbling fluidized bed of small particles. Powder Technology 110, 158–168.

49 Zhang, J., Li, Y., Fan, L.-S., 2000. Numerical studies of bubble and particle dynamics in a three-phase fluidized bed at elevated pressures. Powder Technology 112, 46–56.

50 Rhodes, M.J., Wang, X.S., Nguyen, M., Stewart, P., Liffman, K., 2001. Study of mixing in gas-fluidized beds using a DEM model. Chemical Engineering Science 56, 2859–2866.

51 Wang, X.S., Rhodes, M.J., 2003. Determination of particle residence time at the walls of gas fluidized beds by discrete element method simulation.Chemical Engineering Science 58, 387–395.

52. Yu, A.B., Xu, B.H., 2003. Particle scale modelling of particle–fluid flow in fluidization. Journal of Chemical Technology and Biotechnology 78, 111–121.
53. Cundall, P.A., Strack, O.D.L., 1979. A discrete numerical model for granular assemblies. Geotechnique 29, 47–65.
54. Di Felice, R., 1994. The voidage function for .uid–particle interaction systems. International Journal of Multiphase Flow 20, 153–159.
55. Gidaspow, D., 1994. Multiphase Flow and Fluidization. Academic Press, San Diego.
56. S.Barghi,C.L.Briens,M.A.Bengoughou,2003.Mixing and segregation of binary mixturesof particlesin liquid-solid fluidized bed. Powder Technology, 223~233
57. L.G. Gibilaro, I. Hossain, S.P. Waldram, Chem. Eng. Sci. 40 (12) (1985) 2233–2238.
58. N. Epstein, B. Leclair, Chem. Eng. Sci. 40 (1985) 1517–1526.
59. Y. Kang, J.B. Nah, B.T. Min, Chem. Eng. Commun. 97 (1990) 197– 208.
60. A. Mohammad, J. Peterson, AIChE J. 39 (9) (1993) 1465.
61. M.R. Al-Dobbin, J. Garside, Trans. Inst. Chem. Eng. 57 (1979) 94
62. A.K.A. Juma, J.F. Richardson, Chem. Eng. Sci. 38 (1983) 955
63. T. Matsumoto, N. Hidaka, H. Takenouchi, S. Morooka, Powder Technol.68 (1991) 131.
64. J.M. Coulson, J.F. Richardson (Eds.), Chemical Engineering, vol. 2, Pergamon, Oxford, 1968.
65. W.K.Lewis,E.R.Gililand,W.C.Bauer, Ind.Eng.Chem.41(1949)1104.
66. R. Hoffman, L. Lapidus, J.C. Elgin, AIChE J. 6 (1960) 321.
67. N.G. Stanley-Wood, E. Obata, Powder Technol. 60 (1990) 61– 70.
68. S. Barghi, Segregation and defluidized zones in fluidized beds, PhD Thesis, University of Western Ontario, London, Canada, October 1997.
69. S. Barghi, C.L. Briens, Can. J. Chem. Eng. 79 (2001) 430– 437
70. H. Han, S.D. Kim, Radial dispersion and bubble characteristics in three-phase fluidized beds, Chem. Eng. Commun. 94 (1990) 9– 26.
71 M. Wirsum, F. Fett, N. Iwanova, G. Lukjanow, Powder Technol.(2001) 63– 69.
72 D. Abellon, Z.I. Kolar, W. den Hollander, J.J.M. de Goeij, J.C. Schouten, C.M. Van den Bleek, Powder Technol. 92 (1997) 53.
73 Yu.S. Teplitskii, V.I. Kovenskii, E.F. Nogotov z, V.A. Borodulya, International Journal of Heat and Mass Transfer 49 (2006) 4183–4193
74 A.P. Baskakov, in: V.G. Ainshtein, A.P. Baskakov (Eds.), Fluidization, Khimiya,

Moscow, pp. 333–395

75 Yu.S. Teplitskii, V.A. Borodulya, E.F. Nogotov, Axial solids in a circulating fluidized Int. J. Heat Mass Transfer 46 (2003) 4335-4343

76 F. Wei, Z. Wang, Y. Jin, et al., Dispersion of lateral and axial solids in a cocurrent down- flow circulating fluidized bed, Powder Technol. 81 (1994) 25–30.

77 G.S. Patience, J. Chaouki, Solids hydrodynamics in the fully developed region of CFB risers, in: Proceedings of the Eighth Engineering Foundational Conference on fluidization, Tours, 1995, vol. 1, pp. 33– 40.

78 Laihong Shen, Mingyao Zhang, Yiqian Xu, Powder Technology 84 (1995) 207-212

79 D. Kunii and O. Levenspiel, *Fluidization Engineering,* Wiley, New York, 1969

80 Bing Du,Fei Wei, chemical engg and processing,41(2002)329-325

81 G.Grasa, J.C.Abanades**,** Chemical Engineering Science ,57(2002) 2791-2798

82 I. Eames, M.A. Gilbertson, Powder Technology 154 (2005) 185 – 193

83 L. Shen, M. Zhang, Y. Xu, Solids mixing in fluidized beds, Powder Technol. 84 (1995) 207– 212.

84 L. Shen, M. Zhang, Effect of particle size on solids mixing in bubbling fluidized beds, Powder Technol. 97 (1998) 170–177.

85 L. Shen, M. Zhang, Y. Xu, Model for solids mixing in a twodimensional gas-fluidized bed, Chem. Eng. Sci. 50 (1995) 1841–1844.

86 L. Fan, J.C. Song, N. Yutani, Radial particle mixing in gas– solids fluidized beds, Chem. Eng. Sci. 41 (1986) 117– 122.

87 G. Batchelor, J. Nitsche, The expulsion of particles from a buoyant blob in a fluidized Bed, J. Fluid Mech. 278 (1994) 63– 81

88 A Kumar, Prof (Dr) G K Roy, Institute of Engineers-India chemical engg division vol 84(march 2004) 55-58.

89 Kono and M Jinnai. ëThe Influence of Baffle Design on Fluidization Characteristics in a Fluid Bed Unit System.í A I Ch E Symposium Series, vol 80, no 241, 1983, p 169

90 J Zhao Xiaogang and X Heqing. ëStudy on Bubble Behaviour in Fluidized Bed with Perforated Baffles.í Journal of Huaxue Fanying Gongcheng Yu Gongyi, vol 8, no 1, 1992, p 54.

91 T Miyahara Tsuchiya and L S Fan. ëVisualization of Bubble-wake Interaction for a

Strem of Bubbles in a Two-dimensional Liquid-solid Fluidized Bed. International . Journal of Multiphase Flow, vol 15, no 1, 1989, p 35

92 J Baeyens and D Geldart. ëAn Investigation into Slugging Fluidized Beds.' Chemical Engineering Science, vol 29, 1974, p 255.

93 J.J.Van Deemter, process instrument symptom on fluidization,A.A.H . drinkenburfg,ed, Netherlands University press, Amsterdam, 1967,p-334

94 Kunii, D. and Levenspeiel ,o. , “Fluidization Engg”, Butterworth-Heineman, oneham, USA,(1991)

95 Brotz,W.,Chemical eng. Tech 28(1956)165.

96 P.M.Heertjes, L.H.de Nie and J. Verloop, in proc. Int. symp. On fluidization A.A.H,drinkenburg, ed p 476,Netherland &University press,Amsterdam,1967

97 T.Hirama,M.Ishida, andT. Shirai,Kagaku Ronbunshu,1,272(1975).

98 Y.Shi and M.Gu in proc.3rd World congress, chemical engineering,Tokyo,1986

99 D.Bellgardt and J.Wertha, inproc.16th Int. Symp. On Heat and Mass Transfer, Durovnik,1984

100 S.S.Sastry,Introductory methods of Numerical Analysys,3rd Edition,page 222-223,266-268.

Appendix-1

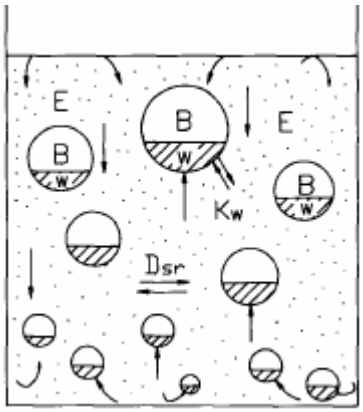

[Figure -1, Mechanistic model of a gas-solid fluidized bed.]

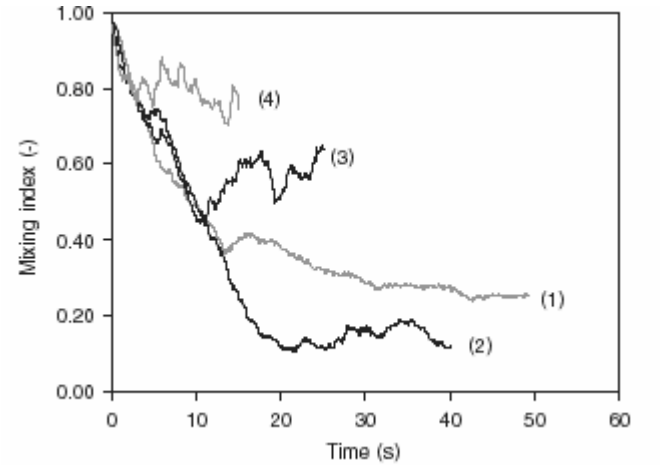

Figure-2, Variation of mixing index with time when gas velocity is 0.8m/s (line 1); 1.0 m/s (line 2); 1.2 m/s (line 3); 1.4 m/s (line 4)

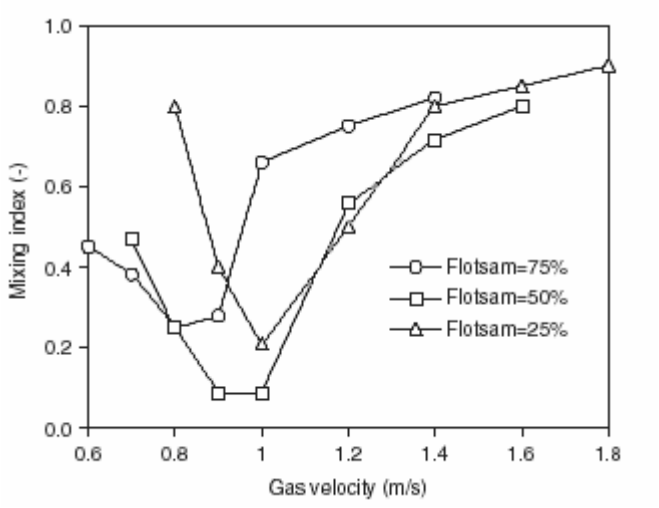

Figure- 3, Mixing Index as a function of gas velocity for different volume fraction of flotsam in a mixture

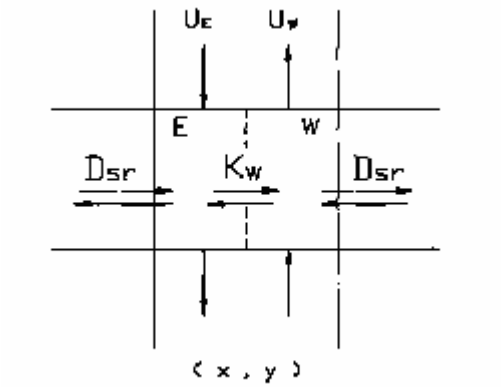

Figure -4, Schematic mass balance of the tracers in emulsion and wake solids

Experimental Setup:

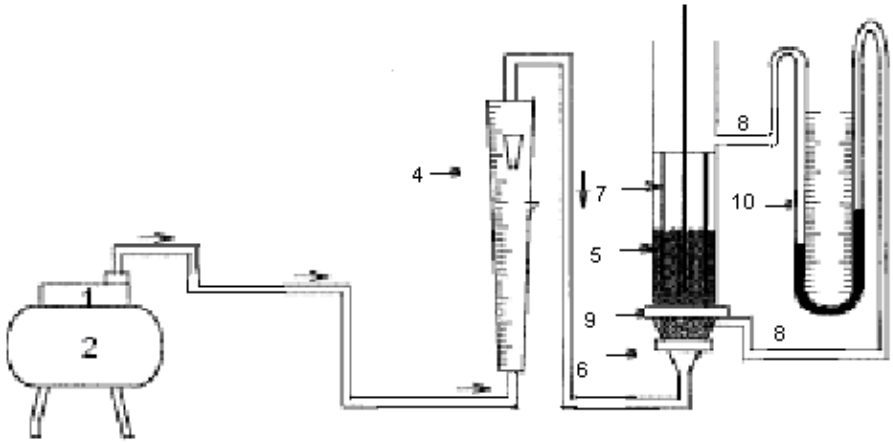

Fig. 5 : Experimental set-up for the fluidized bed

The experimental set up broadly consists of the following parts,

1. Compressor
2. Receiver
3. Constant pressure tank
4. Rotameter
5. Fluidizer with bed (i.e. fluidized bed)
6. Calming section with glass beads
7. Promoter
8. Pressure tappings
9. Distributor
10. Manometer

Appendix-2

Table-1

SIZE OF MATERIAL	DIAMETER OF SAGO	MINIMUM FLUIDISATION VELOCITY OF SAGO	DENSITY
SMALLER SIZE SAGO	1.355mm	0.465 m/s	1304 KG/ m^3
BIGGER SIZE SAGO	3.375mm	1.0335 m/s	1304 KG/ m^3

Appendix-3

2.1 STATIC BED HEIGHT=24CM

2.1.1. STATIC BED CONDITION

W=2.791 KG, ROTAMETER READING =28 m^3 /hr

SL NO.	BED HEIGHT IN cm	EXPERIMENTAL MIXING INDEX VALUE	THEORITICAL MIXING INDEX VALUE	PERCENTAGE OF ERROR
1	4	1.0624	0.668	37.123
2	6	1.0508	0.617	41.282
3	8	1.048	0.606	42.175
4	10	1.0464	0.604	42.278
5	12	1.0396	0.602	42.093
6	14	1.0392	0.607	41.589
7	16	1.0204	0.594	41.787
8	18	1.0048	0.630	37.30
9	20	0.958	0.527	44.989

2.1.2 FLUIDIZED BED

WEIGHT=3 KG, ROTAMETER READING=37 m^3 /hr

SL NO.	BED HEIGHT IN cm	EXPERIMENTAL MIXING INDEX VALUE	THEORITICAL MIXING INDEX VALUE	PERCENTAGE OF ERROR
1	4	0.7624	0.625	18.02
2	6	0.6668	0.594	10.91
3	8	0.65	0.589	9.38
4	10	0.61	0.588	3.6
5	12	0.5224	0.588	-12.55
6	14	0.5	0.589	-17.8

2.1.3. FLUIDISED BED WITH ROD PROMOTER

WEIGHT=3 KG, ROTAMETER READING =34 m^3 /hr

SL NO.	BED HEIGHT IN cm	EXPERIMENTAL MIXING INDEX VALUE	THEORITICAL MIXING INDEX VALUE	PERCENTAGE OF ERROR
1	4	0.7476	0.658	11.985
2	6	0.7384	0.608	17.66
3	8	0.7308	0.597	18.308
4	10	0.652	0.596	8.58
5	12	0.588	0.593	-0.8
6	14	0.57	0.598	-4.9
7	16	0.5524	0.583	-5.5
8	18	0.5304	0.624	-17.64
9	20	0.5128	0.514	-0.23

2.1.4. FLUIDISED BED WITH DISC PROMOTER

WEIGHT=3 KG, ROTAMETER READING =30 m^3 /hr

SL NO.	BED HEIGHT IN cm	EXPERIMENTAL MIXING INDEX VALUE	THEORITICAL MIXING INDEX VALUE	PERCENTAGE OF ERROR
1	4	0.8984	0.663	26.2
2	6	0.832	0.612	26.4
3	8	0.7816	0.601	23.1
4	10	0.7768	0.6	22.76
5	12	0.73424	0.597	18.69
6	14	0.7056	0.602	14.68
7	16	0.7024	0.588	16.28
8	18	0.64224	0.627	2.37
9	20	0.6168	0.520	15.7

2.1.5. FLUIDISED BED WITH DISC PROMOTER WITH STIRRING

WEIGHT=3 KG, ROTAMETER READING = 72 m^3 /hr

SL NO.	BED HEIGHT IN cm	EXPERIMENTAL MIXING INDEX VALUE	THEORITICAL MIXING INDEX VALUE	PERCENTAGE OF ERROR
1	4	0.9264	0.671	27.56
2	6	0.8448	0.621	26.5
3	8	0.7792	0.609	21.84
4	10	0.6788	0.607	10.57
5	12	0.6036	0.605	-0.23
6	14	0.5496	0.610	-10.98
7	16	0.5724	0.597	-4.29
8	18	0.5556	0.633	-13.93
9	20	0.554	0.532	3.97

2.1.6. FLUIDISED BED WITH ROD PROMOTER WITH STIRRING

WEIGHT=3.2 KG, ROTAMETER READING = 89 m^3 /hr

SL NO.	BED HEIGHT IN cm	EXPERIMENTAL MIXING INDEX VALUE	THEORITICAL MIXING INDEX VALUE	PERCENTAGE OF ERROR
1	4	0.8776	0.561	36.03
2	6	0.6604	0.552	16.41
3	8	0.58	0.551	5.0
4	10	0.53	0.551	-3.9
5	12	0.5212	0.551	-5.7
6	14	0.432	0.552	-27.7

2.2 STATIC BED HEIGHT =20 CM

2 .2.1. STATIC BED

WEIGHT=2.64 KG, ROTAMETER READING = 58 m^3 /hr

SL NO.	BED HEIGHT IN cm	EXPERIMENTAL MIXING INDEX VALUE	THEORITICAL MIXING INDEX VALUE	PERCENTAGE OF ERROR
1	4	1.1776	0.748	36.44
2	6	1.1696	0.662	43.4
3	8	1.1004	0.626	41.45
4	10	1.0684	0.629	39.94
5	12	1.048	0.603	42.46
6	14	1.04	0.644	38.07
7	16	1.0272	0.565	44.98
8	18	.9988	0.712	28.71

2.2.2. FLUIDISED BED

WEIGHT=2.64 KG, ROTAMETER READING = 56 m^3 /hr

SL NO.	BED HEIGHT IN cm	EXPERIMENTAL MIXING INDEX VALUE	THEORITICAL MIXING INDEX VALUE	PERCENTAGE OF ERROR
1	4	0.8648	0.685	20.79
2	6	0.854	0.623	27.04
3	8	0.8372	0.606	27.61
4	10	0.8164	0.604	26.01
5	12	0.80	0.599	25.12
6	14	0.6808	0.609	10.54
7	16	0.6568	0.584	11.08
8	18	0.5896	0.644	-9.22
9	20	0.4252	0.498	-17.12

2.2.3. FLUIDISED BED WITH ROD PROMOTER

WEIGHT=2.64 KG, ROTAMETER READING = 80 m^3 /hr

SL NO.	BED HEIGHT IN cm	EXPERIMENTAL MIXING INDEX VALUE	THEORITICAL MIXING INDEX VALUE	PERCENTAGE OF ERROR
1	4	0.887	0.909	-2.4
2	6	0.8628	0.864	-0.14
3	8	0.8333	0.766	8.04
4	10	0.8288	0.815	1.66
5	12	0.7728	0.698	9.67
6	14	0.7224	0.852	-17.94
7	16	0.71	0.609	14.22
8	18	0.6224	0.907	-45.72
9	20	0.5592	0.422	24.53

]

2.2.4. FLUIDISED BED WITH DISC PROMOTER

WEIGHT=2.64 KG, ROTAMETER READING = 65.5 m^3 /hr

SL NO.	BED HEIGHT IN cm	EXPERIMENTAL MIXING INDEX VALUE	THEORITICAL MIXING INDEX VALUE	PERCENTAGE OF ERROR
1	4	0.9404	0.759	19.28
2	6	0.877	0.685	21.89
3	8	0.8744	0.662	24.3
4	10	0.856	0.656	23.36
5	12	0.8104	0.648	20.04
6	14	0.746	0.660	11.52
7	16	0.3372	0.631	-87.12
8	18	0.66	0.698	-5.7
9	20	0.6236	0.537	13.88

2.2.5. FLUIDISED BED WITH DISC PROMOTER WITH STIRRING

WEIGHT=2.849 KG, ROTAMETER READING = 75 m^3 /hr

SL NO.	BED HEIGHT IN cm	EXPERIMENTAL MIXING INDEX VALUE	THEORITICAL MIXING INDEX VALUE	PERCENTAGE OF ERROR
1	4	0.7504	0.709	5.5
2	6	0.686	0.644	6.12
3	8	0.6588	0.626	4.97
4	10	0.63264	0.623	1.5
5	12	0.5884	0.618	-5.03
6	14	0.586	0.627	-7.0
7	16	0.5784	0.604	-4.42
8	18	0.502	0.660	-31.47
9	20	0.3844	0.520	-35.27

2.2.6. FLUIDISED BED WITH ROD PROMOTER WITH STIRRING

WEIGHT=2.849 KG, ROTAMETER READING = 88 m^3 /hr

SL NO.	BED HEIGHT IN cm	EXPERIMENTAL MIXING INDEX VALUE	THEORITICAL MIXING INDEX VALUE	PERCENTAGE OF ERROR
1	4	0.7896	0.834	-5.6
2	6	0.7716	0.747	3.18
3	8	0.71	0.703	0.98
4	10	0.698	0.702	-0.57
5	12	0.685	0.672	1.89
6	14	0.6616	0.715	-8.07
7	16	0.622	0.629	-1.125
8	18	0.5678	0.788	-38.78

2.3 STATIC BED HEIGHT =16 CM

2.3.1 STATIC BED

WEIGHT=2.083 KG, ROTAMETER READING=60 m^3 /hr

SL NO.	BED HEIGHT IN cm	EXPERIMENTAL MIXING INDEX VALUE	THEORITICAL MIXING INDEX VALUE	PERCENTAGE OF ERROR
1	4	1.3432	0.841	37.37
2	6	1.2224	0.754	38.3
3	8	1.172	0.707	39.67
4	10	1.17	0.7078	39.57
5	12	1.05923	0.673	36.45
6	14	1.056	0.722	31.62

2.3.2 FLUIDISED BED

WEIGHT=2.083 KG, ROTAMETER READING=60 m^3 /hr

SL NO.	BED HEIGHT IN cm	EXPERIMENTAL MIXING INDEX VALUE	THEORITICAL MIXING INDEX VALUE	PERCENTAGE OF ERROR
1	4	1.0626	0.841	20.8
2	6	1.06	0.755	28.77
3	8	1.0468	0.7083	32.28
4	10	1.0256	0.7086	30.86
5	12	0.907	0.674	25.68
6	14	0.902	0.723	19.84
7	16	0.8358	0.629	24.74
8	18	0.7657	0.800	-4.48
9	20	0.7	0.484	30.85

2.3.3 FLUIDISED BED WITH DISC PROMOTER

WEIGHT=2.083 KG, ROTAMETER READING=44 m^3 /hr

SL NO.	BED HEIGHT IN cm	EXPERIMENTAL MIXING INDEX VALUE	THEORITICAL MIXING INDEX VALUE	PERCENTAGE OF ERROR
1	4	1.426	0.826	42.07
2	6	1.376	0.738	46.36
3	8	1.1304	0.690	38.96
4	10	1.1268	0.693	38.45
5	12	1.0476	0.657	37.24
6	14	1.0072	0.709	29.6
7	16	0.9816	0.610	37.85
8	18	0.965	0.787	18.44

2.3.4. FLUIDISED BED WITH ROD PROMOTER

WEIGHT=2.083 KG, ROTAMETER READING=43.5 m^3 /hr

SL NO.	BED HEIGHT IN cm	EXPERIMENTAL MIXING INDEX VALUE	THEORITICAL MIXING INDEX VALUE	PERCENTAGE OF ERROR
1	4	1.978	0.821	58.5
2	6	1.4322	0.733	48.81
3	8	1.399	0.687	50.9
4	10	1.345	0.688	48.84
5	12	1.3386	0.654	51.14
6	14	1.166	0.704	39.62
7	16	1.125	0.609	45.86
8	18	1.091	0.781	28.41
9	20	.8222	0.467	43.18

2.3.5 FLUIDISED BED WITH DISC PROMOTER WITH STIRRING

WEIGHT=2.325 KG, ROTAMETER READING=71 m^3 /hr

SL NO.	BED HEIGHT IN cm	EXPERIMENTAL MIXING INDEX VALUE	THEORITICAL MIXING INDEX VALUE	PERCENTAGE OF ERROR
1	4	0.882	0.621	29.6
2	6	0.80064	0.591	26.18
3	8	0.7748	0.586	24.36
4	10	0.7412	0.5856	21.0
5	12	0.732	0.5850	20.08
6	14	0.676	0.5868	13.19
7	16	0.6692	0.5807	13.22
8	18	0.6668	0.6010	9.8
9	20	0.6412	0.533	16.87

2.3.6 FLUIDISED BED WITH ROD PROMOTER WITH STIRRING

WEIGHT=2.325 KG, ROTAMETER READING=73 m^3 /hr

SL NO.	BED HEIGHT IN cm	EXPERIMENTAL MIXING INDEX VALUE	THEORITICAL MIXING INDEX VALUE	PERCENTAGE OF ERROR
1	4	0.768	0.816	-6.25
2	6	0.7572	0.728	3.85
3	8	0.732	0.681	6.97
4	10	0.6192	0.684	-10.46
5	12	0.586	0.648	-10.58
6	14	0.5688	0.701	-23.24
7	16	0.5424	0.602	-10.98

2.4 STATIC BED HEIGHT=12CM

2.4.1 STATIC BED

WEIGHT=1.597 KG, ROTAMETER READING=33 m^3 /hr

SL NO.	BED HEIGHT IN cm	EXPERIMENTAL MIXING INDEX VALUE	THEORITICAL MIXING INDEX VALUE	PERCENTAGE OF ERROR
1	4	1.2568	0.835	33.51
2	6	1.14048	0.7493	39.07
3	8	1.13304	0.6947	38.68
4	10	0.962	0.702	27.02

2.4.2 FLUIDISED BED

WEIGHT=1.597 KG, ROTAMETER READING = 40 m^3 /hr

SL NO.	BED HEIGHT IN cm	EXPERIMENTAL MIXING INDEX VALUE	THEORITICAL MIXING INDEX VALUE	PERCENTAGE OF ERROR
1	4	1.1644	0.854	26.65
2	6	1.11	0.774	30.27
3	8	1.05	0.704	32.95
4	10	0.9768	0.725	25.77
5	12	0.9376	0.654	30.24
6	14	0.8736	0.752	13.91

2.4.3 FLUIDISED BED WITH ROD PROMOTER

WEIGHT=1.597 KG, ROTAMETER READING = 44 m^3 /hr

SL NO.	BED HEIGHT IN cm	EXPERIMENTAL MIXING INDEX VALUE	THEORITICAL MIXING INDEX VALUE	PERCENTAGE OF ERROR
1	4	1.961	0.821	58.1
2	6	1.7108	0.735	57.01
3	8	1.6714	0.672	59.78
4	10	1.5384	0.689	55.21
5	12	1.4648	0.628	57.1
6	14	1.27	0.715	43.7
7	16	1.0128	0.566	44.07

2.4. 4 FLUIDISED BED WITH DISC PROMOTER

WEIGHT=1.597 KG, ROTAMETER READING = 39 m^3 /hr

SL NO.	BED HEIGHT IN cm	EXPERIMENTAL MIXING INDEX VALUE	THEORITICAL MIXING INDEX VALUE	PERCENTAGE OF ERROR
1	4	1.444	0.847	41.34
2	6	1.0768	0.765	28.90
3	8	0.9784	0.699	28.55
4	10	0.59	0.716	-21.3
5	12	0.3844	0.652	-69.61

2.4.5 FLUIDISED BED WITH DISC PROMOTER WITH STIRRING

WEIGHT=1.597 KG, ROTAMETER READING = 39 m^3 /hr

SL NO.	BED HEIGHT IN cm	EXPERIMENTAL MIXING INDEX VALUE	THEORITICAL MIXING INDEX VALUE	PERCENTAGE OF ERROR
1	4	0.9076	0.814	10.31
2	6	0.7772	0.726	6.58
3	8	0.651	0.680	-4.45
4	10	0.6216	0.682	-9.81
5	12	0.5914	0.647	-9.4
6	14	0.5656	0.699	-23.58
7	16	0.5516	0.602	-9.13

2.4.6 FLUIDISED BED WITH ROD PROMOTER WITH STIRRING

WEIGHT=1.597 KG, ROTAMETER READING = 70 m^3 /hr

SL NO.	BED HEIGHT IN cm	EXPERIMENTAL MIXING INDEX VALUE	THEORITICAL MIXING INDEX VALUE	PERCENTAGE OF ERROR
1	4	0.8332	0.715	14.18
2	6	0.7876	0.650	17.47
3	8	0.7733	0.632	18.27
4	10	0.7712	0.629	18.43
5	12	0.7612	0.624	18.02
6	14	0.6873	0.632	8.04
7	16	0.68364	0.612	10.47
8	18	0.6308	0.664	-5.2
9	20	0.6064	0.530	12.6

2.5 VELOCITY=0.862 m/s,Hs=20cm

2.5.1 STATIC BED

WEIGHT=2.5 KG, ROTAMETER READING = 42 m^3 /hr

SL NO.	BED HEIGHT IN cm	EXPERIMENTAL MIXING INDEX VALUE	THEORITICAL MIXING INDEX VALUE	PERCENTAGE OF ERROR
1	4	1.293	0.811	37.27
2	6	1.27	0.723	43.07
3	8	1.23	0.680	44.71
4	10	1.225	0.680	44.48
5	12	1.214	0.650	46.45
6	14	1.05	0.695	33.8
7	16	0.94	0.608	35.31
8	18	0.855	0.767	10.29

2.5.2 FLUIDISED BED

WEIGHT=2.5 KG, ROTAMETER READING = 42 m^3 /hr

SL NO.	BED HEIGHT IN cm	EXPERIMENTAL MIXING INDEX VALUE	THEORITICAL MIXING INDEX VALUE	PERCENTAGE OF ERROR
1	4	1.1548	0.818	29.11
2	6	1.112	0.811	27.06
3	8	1.0948	0.724	33.82
4	10	1.0864	0.681	37.3
5	12	1.0755	0.6811	36.67
6	14	1.024	0.651	36.64
7	16	0.9624	0.695	27.78
8	18	0.9608	0.609	36.61
9	20	0.89336	0.767	14.14

2.5.3 FLUIDISED BED WITH ROD PROMOTER

WEIGHT=2.5 KG, ROTAMETER READING = 42 m^3 /hr

SL NO.	BED HEIGHT IN cm	EXPERIMENTAL MIXING INDEX VALUE	THEORITICAL MIXING INDEX VALUE	PERCENTAGE OF ERROR
1	4	1.0104	0.818	19.01
2	6	0.97	0.811	16.4
3	8	0.96	0.724	24.58
4	10	0.8376	0.681	18.63
5	12	0.8312	0.6811	18.05
6	14	0.8	0.651	18.62
7	16	0.7656	0.695	9.15
8	18	0.661	0.609	7.86

2.5.4 FLUIDISED BED WITH DISC PROMOTER

WEIGHT=2.5 KG, ROTAMETER READING = 42 m^3 /hr

SL NO.	BED HEIGHT IN cm	EXPERIMENTAL MIXING INDEX VALUE	THEORITICAL MIXING INDEX VALUE	PERCENTAGE OF ERROR
1	4	1.1292	0.818	27.54
2	6	0.8292	0.811	2.19
3	8	0.6684	0.724	-8.31
4	10	0.664	0.681	-2.56
5	12	0.6104	0.6811	-11.65
6	14	0.5672	0.651	-14.81
7	16	0.5068	0.695	-18.82
8	18	0.486	0.609	-25.3

2.5.5 FLUIDISED BED WITH ROD PROMOTER WITH STIRRING

WEIGHT=2.6 KG, ROTAMETER READING = 42 m^3 /hr

SL NO.	BED HEIGHT IN cm	EXPERIMENTAL MIXING INDEX VALUE	THEORITICAL MIXING INDEX VALUE	PERCENTAGE OF ERROR
1	4	1.703	0.703	58.71
2	6	1.00734	0.641	36.34
3	8	0.8821	0.624	29.25
4	10	0.63803	0.622	2.5
5	12	0.56025	0.618	-10.31
6	14	0.555	0.625	-12.61
7	16	0.41214	0.605	-46.84
8	18	0.4038	0.655	-62.2

2.6 VELOCITY=1.027m/s

2.6.1 STATIC BED

WEIGHT=2.5 KG, ROTAMETER READING = 50 m^3 /hr

SL NO.	BED HEIGHT IN cm	EXPERIMENTAL MIXING INDEX VALUE	THEORITICAL MIXING INDEX VALUE	PERCENTAGE OF ERROR
1	4	1.2872	0.757	41.18
2	6	1.2684	0.672	47.07
3	8	1.2656	0.637	49.66
4	10	1.206	0.638	47.09
5	12	1.0968	0.615	43.88
6	14	1.0168	0.651	35.92
7	16	0.9745	0.581	40.34
8	18	0.7725	0.715	7.44
9	20			

2.6.2 FLUIDISED BED

WEIGHT=2.5 KG, ROTAMETER READING = 50 m^3 /hr

SL NO.	BED HEIGHT IN cm	EXPERIMENTAL MIXING INDEX VALUE	THEORITICAL MIXING INDEX VALUE	PERCENTAGE OF ERROR
1	4	0.9828	0.787	19.92
2	6	0.982	0.703	28.41
3	8	0.9488	0.671	29.27
4	10	0.8744	0.667	23.71
5	12	0.8736	0.651	25.48
6	14	0.83304	0.675	18.96
7	16	0.822	0.623	24.20
8	18	0.82024	0.730	9.02
9	20	0.816	0.506	37.9

2.6.3 FLUIDISED BED WITH ROD PROMOTER

WEIGHT=2.5 KG, ROTAMETER READING = 50 m^3 /hr

SL NO.	BED HEIGHT IN cm	EXPERIMENTAL MIXING INDEX VALUE	THEORITICAL MIXING INDEX VALUE	PERCENTAGE OF ERROR
1	4	1.0374	0.781	24.686
2	6	0.9545	0.703	26.34
3	8	0.8581	0.671	21.79
4	10	0.8333	0.667	19.92
5	12	0.8226	0.651	20.86
6	14	0.7911	0.675	14.67
7	16	0.7323	0.623	14.92
8	18	0.6864	0.730	-6.35
9	20	0.576	0.506	12.15

2.6.4 FLUIDISED BED WITH DISC PROMOTER

WEIGHT=2.5 KG, ROTAMETER READING = 50 m^3 /hr

SL NO.	BED HEIGHT IN cm	EXPERIMENTAL MIXING INDEX VALUE	THEORITICAL MIXING INDEX VALUE	PERCENTAGE OF ERROR
1	4	1.025	0.785	23.41
2	6	0.951	0.701	26.28
3	8	0.9202	0.669	27.29
4	10	0.8533	0.665	22.06
5	12	0.7786	0.649	16.64
6	14	0.7667	0.673	12.22
7	16	0.7074	0.620	12.35
8	18	0.6667	0.729	-9.36
9	20	0.4678	0.502	-7.3

2.6.5 FLUIDISED BED WITH ROD PROMOTER WITH STIRRING

WEIGHT=2.6 KG, ROTAMETER READING = 50 m^3 /hr

SL NO.	BED HEIGHT IN cm	EXPERIMENTAL MIXING INDEX VALUE	THEORITICAL MIXING INDEX VALUE	PERCENTAGE OF ERROR
1	4	0.8855	0.644	27.27
2	6	0.8202	0.611	25.5
3	8	0.6998	0.606	13.4
4	10	0.6908	0.605	12.42
5	12	0.6282	0.605	3.7
6	14	0.5708	0.606	-6.16

2.6.6 FLUIDISED BED WITH DISC PROMOTER WITH STIRRING

WEIGHT=2.5 KG, ROTAMETER READING = 50 m^3 /hr

SL NO.	BED HEIGHT IN cm	EXPERIMENTAL MIXING INDEX VALUE	THEORITICAL MIXING INDEX VALUE	PERCENTAGE OF ERROR
1	4	0.8805	0.647	26.51
2	6	0.6478	0.614	5.21
3	8	0.64725	0.609	5.9
4	10	0.5084	0.608	-19.6
5	12	0.4863	0.607	-24.82

2.7 VELOCITY=1.234m/s

2.7.1 STATIC BED

WEIGHT=2.5 KG, ROTAMETER READING = 60 m^3 /hr

SL NO.	BED HEIGHT IN cm	EXPERIMENTAL MIXING INDEX VALUE	THEORITICAL MIXING INDEX VALUE	PERCENTAGE OF ERROR
1	4	1.1768	0.881	25.13
2	6	1.1740	0.837	28.7
3	8	1.0896	0.722	33.7
4	10	1.06	0.787	25.75
5	12	1.024	0.650	36.52
6	14	1.015	0.828	18.42
7	16	0.992	0.559	43.64
8	18	0.9756	0.947	2.93

2.7.2 FLUIDISED BED

WEIGHT=2.5 KG, ROTAMETER READING = 60 m^3 /hr

SL NO.	BED HEIGHT IN cm	EXPERIMENTAL MIXING INDEX VALUE	THEORITICAL MIXING INDEX VALUE	PERCENTAGE OF ERROR
1	4	0.8162	0.775	5.04
2	6	0.7698	0.697	9.45
3	8	0.7572	0.669	11.64
4	10	0.7365	0.664	9.84
5	12	0.7289	0.654	10.27
6	14	0.6931	0.669	3.47
7	16	0.6887	0.633	8.08
8	18	0.6786	0.714	-5.2
9	20	0.5631	0.530	5.87

2.7.3 FLUIDISED BED WITH DISC PROMOTER

WEIGHT=2.5 KG, ROTAMETER READING = 50 m^3 /hr

SL NO.	BED HEIGHT IN cm	EXPERIMENTAL MIXING INDEX VALUE	THEORITICAL MIXING INDEX VALUE	PERCENTAGE OF ERROR
1	4	0.811	0.754	7.02
2	6	0.75984	0.671	11.6
3	8	0.7308	0.639	12.56
4	10	0.7033	0.638	9.28
5	12	0.6972	0.620	11.04
6	14	0.6815	0.649	4.76
7	16	0.575	0.588	-2.26
8	18	0.567	0.708	-24.86
9	20	0.5584	0.469	16.01

2.7.4 FLUIDISED BED WITH ROD PROMOTER

WEIGHT=2.5 KG, ROTAMETER READING = 70 m^3 /hr

SL NO.	BED HEIGHT IN cm	EXPERIMENTAL MIXING INDEX VALUE	THEORITICAL MIXING INDEX VALUE	PERCENTAGE OF ERROR
1	4	0.7267	0.774	-6.5
2	6	0.7	0.695	0.71
3	8	0.6899	0.668	3.1
4	10	0.6753	0.662	1.9
5	12	0.6531	0.653	1.53
6	14	0.609	0.668	-9.6
7	16	0.56985	0.631	-10.74
8	18	0.5567	0.713	-28.07
9	20	0.545	0.527	3.3

2.7.5 FLUIDISED BED WITH ROD PROMOTER WITH STIRRING

WEIGHT=2.6 KG, ROTAMETER READING = 70 m^3 /hr

SL NO.	BED HEIGHT IN cm	EXPERIMENTAL MIXING INDEX VALUE	THEORITICAL MIXING INDEX VALUE	PERCENTAGE OF ERROR
1	4	0.7966	0.751	5.72
2	6	0.7734	0.667	13.75
3	8	0.7667	0.6349	20.75
4	10	0.7535	0.6344	15.8
5	12	0.7352	0.614	16.48
6	14	0.6145	0.646	-5.12
7	16	0.6017	0.582	3.27
8	18	0.5408	0.707	-30.73
9	20	0.3292	0.462	-40.34

2.7.6 FLUIDISED BED WITH DISC PROMOTER WITH STIRRING

WEIGHT=2.486 KG, ROTAMETER READING = 70 m^3 /hr

SL NO.	BED HEIGHT IN cm	EXPERIMENTAL MIXING INDEX VALUE	THEORITICAL MIXING INDEX VALUE	PERCENTAGE OF ERROR
1	4	0.7257	0.774	-6.6
2	6	0.658	0.696	-5.7
3	8	0.556	0.668	20.14
4	10	0.5168	0.663	-28.29
5	12	0.4602	0.653	-41.9
6	14	0.429	0.668	-55.7
7	16	0.3993	0.632	-59.26

Appendix-4

3.1 Tabulation for variation of mixing index with bed height at different static bed height

Fluidized bed with rod promoter condition,Umf=0.465m/s,uj=0.665m/s,f=0.15

Static bed height in cm	MI1 Ht = 0	MI2 Ht = 2 cm	MI3 Ht = 4 cm	MI4 Ht = 6 cm	MI5 Ht = 8 cm	MI6 Ht = 10cm	MI7 Ht =12cm	MI8 Ht = 14cm	MI9 Ht = 16cm	MI10 Ht = 18cm	MI11 Ht = 20cm
12	1.889	0.947	0.698	0.636	0.620	0.617	0.613	0.621	0.600	0.652	0.520
16	1.894	0.950	0.701	0.639	0.622	0.619	0.615	0.623	0.603	0.654	0.522
20	2.033	0.923	0.652	0.590	0.574	0.574	0.565	0.583	0.544	0.628	0.448
24	2.053	0.919	0.646	0.585	0.568	0.569	0.559	0.578	0.536	0.625	0.438

3.2 Tabulation for variation of mixing index with bed height at different fluidization velocity

Fluidized bed condition,Umf=0.465m/s,uj=0.665m/s,f=0.15

Fluidization Velocity In m/s	MI1 Ht = 0	MI2 Ht = 2 cm	MI3 Ht = 4 cm	MI4 Ht = 6 cm	MI5 Ht = 8 cm	MI6 Ht = 10cm	MI7 Ht =12cm	MI8 Ht = 14cm	MI9 Ht = 16cm	MI10 Ht = 18cm	MI11 Ht = 20cm
.862	1.886	0.950	0.702	0.640	0.624	0.621	0.617	0.624	0.604	0.655	0.525
1.027	1.913	0.945	0.692	0.630	0.614	0.611	0.607	0.615	0.593	0.649	0.510
1.234	1.99	0.931	0.666	0.604	0.588	0.587	0.580	0.594	0.562	0.634	0.470

3.3 Tabulation for variation of mixing index with bed height with increase of jetsam particles composition in the mixture

Static bed condition,umf=0.465m/s,uj=0.665m/s,f=0.15

Jetsam Particles composition	MI1 Ht = 0	MI2 Ht = 2 cm	MI3 Ht = 4 cm	MI4 Ht = 6 cm	MI5 Ht = 8 cm	MI6 Ht = 10cm	MI7 Ht =12cm	MI8 Ht = 14cm	MI9 Ht = 16cm	MI10 Ht = 18cm	MI11 Ht = 20cm
25:75	1.941	0.940	0.683	0.620	0.604	0.602	0.597	0.607	0.581	0.643	0.495
40:60	1.26	0.579	0.411	0.372	0.362	0.362	0.357	0.367	0.344	0.394	0.285
50:50	.990	0.466	0.334	0.303	0.295	0.295	0.291	0.298	0.282	0.318	0.237
90:10	.547	0.259	0.187	0.169	0.165	0.164	0.163	0.166	0.158	0.177	0.133

3.4 Tabulation for variation of mixing index with different bed height with increase in fractional value of bed material.

Rod promoted fluidized condition,umf=.465m/s, Uj=.865 m/s

f	MI1	MI2	MI3	MI4	MI5	MI6	MI7	MI8	MI9	MI10	MI11	MI12
.05	2.034	.744	0.613	0.600	0.5993	0.5992	0.5992	0.5993	0.598	0.6031	0.578	0.711
.1	1.985	0.892	0.655	0.605	0.595	0.593	0.590	0.596	0.581	0.622	0.510	0.812
.15	1.871	1.030	0.734	0.650	0.615	0.618	0.592	0.634	0.554	0.702	0.429	0.934
.2	1.686	1.153	0.805	0.737	0.636	0.693	0.576	0.734	0.497	0.840	0.338	1.072
.25	1.374	1.297	0.799	0.891	0.608	0.848	0.507	0.908	0.398	1.028	0.241	1.22

3.5 Tabulation for difference in mixing index in promoted and unpromoted fluidized bed. 25:75 composition of jetsam particles, static bed height =24 cm, umf= 0.865m/s, uj= 0.865m/s, K=0.04

Bed height in cm	Static bed	Fluidized bed	Fluidized bed with rod promoter	Fluidized bed with disc promoter	Fluidized bed with rod promoter with stirring	Fluidized bed with disc promoter with stirring
0	1.949	1.930	1.977	1.965	1.941	1.194
2	0.902	0.906	0.894	0.897	0.903	0.890
4	0.668	0.675	0.658	0.663	0.671	0.652
6	0.617	0.625	0.608	0.612	0.621	0.602
8	0.606	0.613	0.597	0.601	0.609	0.592
10	0.604	0.617	0.596	0.60	0.607	0.590
12	0.602	0.609	0.593	0.597	0.605	0.597
14	0.607	0.613	0.598	0.602	0.610	0.593
16	0.594	0.601	0.583	0.588	0.597	0.577
18	0.630	0.635	0.624	0.627	0.633	0.620
20	0.527	0.537	0.514	0.520	0.532	0.506
22	0.818	0.821	0.813	0.815	0.819	0.811

Appendix-5

A “c – language program” for the developed mathematical model

```
/*Program for calculating concentration of jetsam particles and mixing index at any height of the bed*/
/*by counter mixing dispersion model*/
#include<stdio.h>
#include<math.h>
#include<conio.h>
void main( )
{
FILE *fp;
fp=fopen("Result.doc","a+");
int i,ip1,ip2;
float t=0.77;
float dt=0.14;
float g=9.81;
  float c1,c2,D1,D2,K1,K11,u0,umf,Dsv,MI,W,J;
  float z[12],fu,K,temp,emf,Dsh[12];
float A[12],b[12],alpha[12],k,uj,B,c[12];
float Beta [12];
float y[12];
clrscr( );
printf("How many different value do you want: ");
scanf("%d",&ip1);
ip2=0;
while(ip2<ip1)
{
ip2++;
fprintf(fp,"\n\n\nInput Sequence:\n",ip2);
D1=1.808*pow(dt,1.35)+0.711*pow(g,0.5);
printf("Enter u0,umfvalues");
scanf("%f %f",&u0,&umf);
fprintf(fp,"u0=%f,umf=%f,",u0,umf);
```

```
temp=1+27.2*(u0-umf);
K1=0.853*(pow(temp,0.3333));
D2=D1*pow(K1,0.5);
c1=1.6*pow(dt,1.35)*(u0-umf)-u0+2*umf;
printf("Enter value of emf");
scanf("%f",&emf);
fprintf(fp,"emf=%f,",emf);
K11=(3.0/1600)*(umf*(u0-umf))*(pow(t,2))/emf;
Dsv=0.06+0.1*u0;
z[0]=0;z[1]=0.02;z[2]=0.04;z[3]=0.06;z[4]=0.08;z[5]=0.10;z[6]=0.12;z[7]=0.14;z[8]=0.16;z[
9]=0.18;z[10]=0.20;z[11]=0.22;
for(i=0;i<12;i++)
{
Dsh[i]=(K1*K1*K11*(1+0.0828*z[i]))/((c1+D2*(1+0.0414*z[i])));
}
printf("Enter value of fu");
scanf ("%f",&fu);
fprintf(fp,"fu=%f,",fu);
for(i=0;i<12;i++)
A[i]=fu*Dsv+Dsh[i];
printf("Enter value of K");
scanf("%f",&K);
fprintf(fp,"K=%f,",K);
for(i=0;i<12;i++)
b[i]=8*K-2*A[i];
 printf("Enter value of uj");
 scanf("%f",&uj);
fprintf(fp,"uj=%f,",uj);
printf("\n enter the value of W and J");
scanf("%f%f",&W,&J);
fprintf(fp,"W=%f,J=%f,",W,J);
 B=fu*uj;
 for(i=0;i<12;i++)
 c[i]=A[i]+B;
```

```
 alpha[0]=b[0];
 for(i=1;i<12;i++)
 alpha[i]=b[i]-((A[i]-B)*c[i-1])/alpha[i-1];
 Beta[0]=(4*K)/(8*K-A[0]*2);
 for(i=1;i<12;i++)
 Beta[i]=4*K-((A[i]-B)*Beta[i-1])/alpha[i];
 y[11]=Beta[11];
 for(i=10;i>=0;i--)
 y[i]=Beta[i]-(c[i]*y[i+1])/alpha[i];
 fprintf(fp,"\n%s\n","Value of y[i]");
 for(i=0;i<12;i++)
 {
 printf("\nvalue of y[%d]=%f",(i+1),y[i]);
 fprintf(fp,"y[%d]=%f,",(i+1),y[i]);
 }
fclose(fp);
fp=fopen("Result.doc","a+");
fprintf(fp,"\n%s\n","Value of MI");
//printf("\n%f ,%f ,%f ,",y[0],W,J);

for(i=0;i<12;i++)
{
   MI=y[i]*W/J;
   printf("\nMI[%d]=%f\n",(i+1),MI);
   fprintf(fp,"MI[%d]=%f,",i+1,MI);
}
fclose(fp);
fp=fopen("Result.doc","a+");

getch( );
}
fclose(fp);
}
```